Chemical genetic screen identifies Gapex-5/GAPVD1 and STBD1 as novel AMPK substrates

Ducommun, Serge; Deak, Maria; Zeigerer, Anja; Göransson, Olga; Seitz, Susanne; Collodet, Caterina; Madsen, Agnete Bjerregaard; Jensen, Thomas Elbenhardt; Viollet, Benoit; Foretz, Marc; Gut, Philipp; Sumpton, David; Sakamoto, Kei
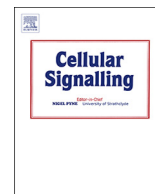
Chemical genetic screen identifies Gapex-5/GAPVD1 and STBD1 as novel AMPK substrates

Serge Ducommun[a,b,1], Maria Deak[a], Anja Zeigerer[c,d,e], Olga Göransson[f], Susanne Seitz[c,d,e], Caterina Collodet[a,b], Agnete B. Madsen[g], Thomas E. Jensen[g], Benoit Viollet[h,i,j], Marc Foretz[h,i,j], Philipp Gut[a], David Sumpton[k], Kei Sakamoto[a,b,*]

[a] Nestlé Research, École Polytechnique Fédérale de Lausanne (EPFL) Innovation Park, bâtiment G, 1015 Lausanne, Switzerland
[b] School of Life Sciences, EPFL, 1015 Lausanne, Switzerland
[c] Institute for Diabetes and Cancer, Helmholtz Center for Environmental Health, 85764 Neuherberg, Germany
[d] Joint Heidelberg-IDC Translational Diabetes Program, Inner Medicine 1, Heidelberg University Hospital, Heidelberg, Germany
[e] German Center for Diabetes Research (DZD), 85764 Neuherberg, Germany
[f] Department of Experimental Medical Sciences, Lund University, 221 84 Lund, Sweden
[g] Department of Nutrition, Exercise and Sports, Faculty of Science, University of Copenhagen, Copenhagen, Denmark
[h] Inserm, U1016, Institut Cochin, Paris, France
[i] CNRS, UMR8104, Paris, France
[j] Université Paris Descartes, Sorbonne Paris cité, Paris, France
[k] Cancer Research UK Beatson Institute, Glasgow G61 1BD, UK

ARTICLE INFO

ABSTRACT

AMP-activated protein kinase (AMPK) is a key regulator of cellular energy homeostasis, acting as a sensor of energy and nutrient status. As such, AMPK is considered a promising drug target for treatment of medical conditions particularly associated with metabolic dysfunctions. To better understand the downstream effectors and physiological consequences of AMPK activation, we have employed a chemical genetic screen in mouse primary hepatocytes in an attempt to identify novel AMPK targets. Treatment of hepatocytes with a potent and specific AMPK activator 991 resulted in identification of 65 proteins phosphorylated upon AMPK activation, which are involved in a variety of cellular processes such as lipid/glycogen metabolism, vesicle trafficking, and cytoskeleton organisation. Further characterisation and validation using mass spectrometry followed by immunoblotting analysis with phosphorylation site-specific antibodies identified AMPK-dependent phosphorylation of Gapex-5 (also known as GTPase-activating protein and VPS9 domain-containing protein 1 (GAPVD1)) on Ser902 in hepatocytes and starch-binding domain 1 (STBD1) on Ser175 in multiple cells/tissues. As new promising roles of AMPK as a key metabolic regulator continue to emerge, the substrates we identified could provide new mechanistic and therapeutic insights into AMPK-activating drugs in the liver.

1. Introduction

AMP-activated protein kinase (AMPK) is a key regulator of cellular energy homeostasis, acting as a sensor of energy and nutrient status through primarily sensing adenine nucleotide levels [1–3]. AMPK is a heterotrimer comprising a catalytic α-subunit and regulatory β- and γ-subunits. Multiple isoforms encoded by distinct genes exist (α1 and α2,

β1 and β2, and γ1, γ2, and γ3), which can theoretically form several distinct heterotrimeric combinations, with the isoform expression profiles varying amongst cells/tissues and also species. Under conditions of cellular energy stress, which leads to an increase in AMP-to-ATP or ADP-to-ATP ratios, AMPK is activated and switches off anabolic processes that consume ATP, while activating catabolic processes that generate ATP in order to restore energy balance [1,2,4–6]. This is

achieved through phosphorylation of a plethora of downstream targets [7], including acetyl CoA carboxylase (ACC) 1 and 2, which modulate lipid synthesis and oxidation, respectively [8,9], TBC1D1, which promotes glucose transport in muscle [10,11], and regulatory-associated protein of mTOR (Raptor), which inhibits protein synthesis and cell growth [12]. More recently, it has been demonstrated that AMPK controls mitochondrial homeostasis and adipose tissue browning through mitochondrial fission factor (MFF) and likely also through targets yet to be identified [13–15]. Due to such key roles that AMPK plays in integrating signalling pathways for maintenance of energy homeostasis, AMPK is considered a promising drug target for treatment of medical conditions associated with the metabolic syndrome, such as insulin resistance and type 2 diabetes [16–19]. However, there is growing evidence that AMPK regulates biological processes not conventionally linked to metabolic processes, including cell division, autophagy, and cell invasion [20–22]. This growing list of emerging roles for AMPK in diverse biological contexts has drawn major attention to AMPK as a drug target for cancer and other diseases. In parallel, however, it has also raised concerns regarding potential side effects, which may arise as a consequence of chronic AMPK activation. To address this, major efforts have been made to understand and design isoform−/complex-specific roles and activators for AMPK, respectively [7,23], and to reveal AMPK substrates and their function [14,20,21,24]. Although various approaches have been developed for identification of AMPK targets, the majority of the studies performed previously utilised immortalised cancer cells or fibroblasts. To better understand the downstream effectors and physiological consequences of AMPK activation, it will be critical to take the cell- and activator-specific context into account.

Hepatic metabolism plays an important role in regulation of whole-body energy balance, as liver is the major site for storage and release of glucose/carbohydrates and for fatty acid synthesis [25]. Several lines of evidence have demonstrated that hepatic AMPK gets activated in response to physiological stimuli, including exercise [26] and nutrient deprivation/starvation [27], and inhibited in response to physio-pathological conditions such as chronic alcohol consumption [28]. Moreover, it is established that antidiabetic drugs, metformin [29,30] and several natural products [31] (e.g. salicylate [32], berberine [33]), robustly activate hepatic AMPK. Collectively, hepatic AMPK has a wider role in coordinating metabolism under various physiological/pathophysiological settings likely through regulating a plethora of downstream targets. In the current study, we have performed a chemical genetic screen in primary hepatocytes to identify new direct targets of AMPK. We report the identification of 65 proteins that are potentially direct targets of AMPK, and we further characterised the phosphorylation sites Ser902 on Gapex-5 (also known as GTPase-activating protein and VPS9 domain-containing protein 1 (GAPVD1)) and Ser175 on starch-binding domain 1 (STBD1).

2. Materials and methods

2.1. Materials

Materials used include 5-aminoimidazole-4-carboxamide riboside (AICAR, A611700; Toronto Research Chemicals), A769662 (S2697; Selleck Chemicals), mass spectrometry grade trypsin (V528A; Promega), creatine kinase (C3755; Sigma), phosphatase inhibitor cocktail 2 and 3 (P5726 and P0044; Sigma), cOmplete protease inhibitor cocktail EDTA-free (11,836,170,001; Roche), p-nitrobenzylmesylate (PNBM; ab138910; Abcam), N^6-(2-Phenylethyl) adenosine-5'-O-(3-thiotriphosphate) (N^6-phenethyl-ATPγS; P 026; Biolog), Protein G Sepharose (P3296; Sigma), FLAG-M2 resin (A2220; Sigma) and NHS-activated Sepharose (17-0906-01; GE Healthcare). 991 (5-[[6-chloro-5-(1-methylindol-5-yl)-1H-benzimidazol-2-yl]oxy]-2-methyl-benzoic acid) (CAS#: 129739-36-2) was described previously [14]. COS-1 (CRL-1650) and AML12 (CRL2254) cell lines were obtained from

American Type Culture Collection. General and specific cell culture reagents were obtained from Thermo Fisher Scientific. All other materials unless otherwise indicated were from Sigma.

2.2. Antibodies

Total acetyl-CoA carboxylase (ACC; #3676), phospho-ACC (S79; #3661), total Raptor (#2280), phospho-Raptor (S792; #2083), total AMPKα (#2532), phospho-AMPKα (T172; #2535), total AMPKβ1 (#4182) and phospho-(S/T) AMPK substrate motif (#5759, lot #7) antibodies were from Cell Signaling Technology. Antibodies against α-tubulin (T6074) and FLAG (F7425) were from Sigma. Antibody against AMPKγ1 was from OriGene Technologies (TA300519), antibodies against thiophosphate-ester were from Abcam (for immunoprecipitation: ab133473; for immunoblot: ab92570), antibodies against Gapex-5 were from Bethyl Laboratories (A302-116A; raised against internal sequence) and Sigma (SAB1401626; raised against N-terminal sequence) and antibodies against STBD1 were a kind gift from Dr. David Stapleton (University of Melbourne; raised against N-terminal peptide 343–358) or obtained from Proteintech Group (11842-1-AP; raised against whole protein). Horseradish peroxidase-conjugated secondary antibodies were from Jackson ImmunoResearch Europe. Site-specific rabbit polyclonal were generated by YenZym Antibodies by immunisation with a phosphorylated peptide of the human sequence (CPERLVRSR-*S-SDIVS-amide for pSer902 Gapex-5, the prefix * denotes the phosphorylated residue) or a combination of two phosphorylated peptides of the human and mouse sequences (CFAEKLP-*S-SNLLKNR-amide and CVAAKLP-*S-SSLLVDR-amide for pSer175 STBD1, CWEMVPRHS-*S-WGDVG-amide and CWEVVSRHS-*S-WGSVG-amide for pSer211 STBD1).

2.3. Animals

Animal studies were approved by the local Ethical Committee of the Canton of Vaud, Switzerland, and performed under license number 2570. C57BL/6N mice were obtained from Charles River Laboratories. Generation of liver-specific AMPKα1/α2 knockout mice has been described previously [34]. Experiments using hepatic AMPKα1/α2 double knockout and its control mice were performed under the approval of the ethics committee from University Paris Descartes (no. CEEA34.BV.157.12) and the French authorisation to experiment on vertebrates (no.75–886) in accordance with the European guidelines. Animal studies for Fig. 4D using C57BL/6 wildtype and muscle-specific KD AMPK overexpressing mice [35] were approved by the Danish Animal Experiments Inspectorate (no. 2016-15-0201-01043).

2.4. Cloning, mutagenesis and adenovirus production

The coding regions of human AMPKα2 (NM_006252), AMPKβ1 (NM_006253) and AMPKγ1 (NM_002733) were amplified from muscle RNA (Agilent) using SuperScript III One-step RT-PCR kit (Thermo Fisher Scientific). Human STBD1 (NM_003943.4) was also amplified from muscle RNA. The resulting PCR products were either ligated into intermediate vector pSC amp/kan (Agilent) or digested with the relevant restriction enzymes and ligated directly into expression vectors. The coding region of human Gapex-5 (NM_001282680.1) was amplified from IMAGE clone 40,083,103 obtained from Source BioScience. Site directed mutagenesis was carried out according to the Quick Change method (Agilent) using KOD polymerase (Novagen). The sequences of all constructs were verified in-house using BigDyeR Terminator 3.1 kit and 3500XL Genetic analyzer (Applied Biosystems).

In order to obtain adenovirus particles the AdEasy vector system was used according to the manufacturer's protocol (Agilent). The coding regions of the different human AMPK subunits (α2, α2-M93G, β1, γ1) were cloned into the intermediate pShuttle-CMV vector, which was transformed into chemically competent BJ5183 E.coli cells carrying the pAdEasy-1 plasmid. The colonies containing the recombinant

plasmids were selected on kanamycin plates and the candidates were verified with restriction digests and by capillary sequencing. The pAdeasy vectors have been packaged using CAP cells derived from human amniocytes by Sirion Biotech.

2.5. General cell culture and mouse primary hepatocytes

AML12 cells were cultured in DMEM/F12 supplemented with 10% foetal calf serum, $1\times$ Insulin-Transferrin-Selenium (ITS G; Gibco 41,400,045) and 100 nM dexamethasone. COS-1 cells were cultured in DMEM supplemented with 10% foetal calf serum. Cells were transfected with DNA using polyethylenimine, treated and harvested 36 h post-transfection. Cells were washed with ice-cold PBS and scraped into lysis buffer (50 mM tris pH 7.5, 1 mM EDTA, 1 mM EGTA, 0.27 M sucrose, 1% (w/v) Triton X-100, 20 mM glycerol-2-phosphate, 50 mM NaF, 5 mM sodium pyrophosphate, 0.5 mM PMSF, 1 mM benzamidine, 1 mM dithiothreitol, 1 mM Na_3VO_4). Lysates were clarified at 3,500 g for 15 min at 4 °C and normalised using Bradford reagent and bovine serum albumin (BSA) as standard.

Primary mouse hepatocytes were isolated from C57BL/6N mice (12–14 weeks old) or from liver-specific AMPKα1/α2 knockout and control mice as previously described [36,37].

2.6. Incubation of isolated mouse skeletal muscle ex vivo

Mice were anaesthetised (6 mg pentobarbital and lidocaine/100 g body weight, intraperitoneal injection) and extensor digitorum longus (EDL) muscles were rapidly removed and mounted on an incubation apparatus. The EDL muscle was incubated in KRH-buffer (supplemented with 2 mM pyruvate, 8 mM mannitol, $1\times$ amino acids (Sigma M5550) and 5 mM Hepes at 30 °C) in the presence of 4 mM AICAR or vehicle for 40 min as previously described [38].

2.7. Immunoprecipitation and immunoblotting

For immunoprecipitation, lysates were incubated with antibody and 5 μl of Protein G Sepharose or 5 μl FLAG-M2 resin on a vibrating platform shaker (1000 rpm) for 16 h at 4 °C. Immunoprecipitate was eluted from the resin by boiling in Laemmli buffer. For Western blotting, cell lysates and tissue homogenates were denatured in Laemmli buffer, separated by SDS-PAGE and transferred to nitrocellulose membrane. Membranes were blocked for 1 h in 20 mM tris (pH 7.6), 137 mM NaCl, 0.1% (v/v) Tween-20 (TBST) containing 5% (w/v) skimmed milk. Membranes were incubated in primary antibody prepared in TBST containing 1% (w/v) BSA overnight at 4 °C. Detection was performed using horseradish peroxidase-conjugated secondary antibodies and enhanced chemiluminescence reagent.

2.8. Substrate screen in cells using ATP-analogue specific AMPK

Primary mouse hepatocytes were isolated and plated on collagen-coated 10-cm dishes at a density of 5×10^6 cells per dish as described above. 5 h after plating, cells were switched to overnight medium. 1 h later, cells were transduced with adenovirus for AMPKα2 (WT or M93G), AMPKβ1 and AMPKγ1 (multiplicity of infection (MOI) of 1 for each AMPK subunit). 16 h after starting transduction, dishes were washed twice with warm PBS and fresh overnight medium was added. 6 h later, cells were washed twice in warm PBS and AMPK substrate labelling with ATPγS analogue was performed [20]. Labelling was performed in 20 mM Hepes pH 7.4 buffer containing 100 mM KOAc, 5 mM NaOAc, 2 mM Mg(OAc)$_2$, 1 mM EGTA, 10 mM MgCl$_2$, 0.5 mM DTT, 5 mM creatine phosphate, 50 μg/ml creatine kinase, 20 μg/ml digitonin, 3 mM GTP, 0.1 mM ATP, 0.1 mM N^6-phenethyl-ATPγS, $1\times$ phosphatase inhibitor cocktails 2 and 3, and $1\times$ cOmplete protease inhibitor. Additionally, 30 μM 991 was added to the labelling buffer to activate AMPK. Cells were labelled during 20 min at room temperature while gently shaking. The labelling reaction was stopped by adding 20 mM EDTA and cells were lysed by adding 1% (w/v) Triton X-100, followed by vortexing and sonication for 30 s. Lysates were then cleared by centrifugation at 3,500 g for 15 min. Lysates were alkylated for 1 h at room temperature on a shaker (1400 rpm) using 2.5 mM PNBM. The buffer was then exchanged to RIPA buffer (50 mM tris pH 7.4, 150 mM NaCl, 1 mM EDTA, 1% (w/v) Triton X-100, 0.5% (w/v) sodium deoxycholate, 0.1% (w/v) sodium dodecyl sulfate (SDS), 20 mM glycerol-2-phosphate, 2.5 mM sodium pyrophosphate, 0.5 mM PMSF, 1 mM benzamidine, and 1 mM Na_3VO_4) using a Sephadex G-25 column. Samples were then immunoprecipitated using anti-thiophosphate ester antibody or rabbit IgG control antibody cross-linked to NHS-activated Sepharose according to the manufacturer's instructions.

2.9. Trypsin digestion and MS analysis

Immunoprecipitated proteins were denatured in Laemmli buffer, alkylated using iodoacetamide and separated by SDS-PAGE on NuPAGE 4–12% bis-tris gels (Thermo Fisher Scientific). Gels were stained with colloidal Coomassie and regions of interest were excised. Gel pieces were destained by successive washing (10 min, 30 °C) in water, 50% acetonitrile, 0.1 M triethylammonium bicarbonate (TEAB, pH 8.5) and 50 mM TEAB in 50% acetonitrile. Gel pieces were dehydrated in 100% acetonitrile and dried before rehydration in 25 mM TEAB containing 5 μg/ml trypsin for 16 h (30 °C). The digestion products were then extracted sequentially with one volume of 100% acetonitrile (15 min, 30 °C) and one volume of 25% acetonitrile and 1.25% formic acid (15 min, 30 °C). The resulting supernatants were pooled and dried. Peptides were re-dissolved in 5% acetonitrile / 0.25% formic acid. Reversed-phase liquid chromatography tandem MS (RPLC-MS/MS) analysis was performed on a LTQ-Orbitrap Velos coupled to a Proxeon Easy-LC. The peptide mixtures were loaded onto a C18 guard column (1.9 μm; 0.1 × 20 mm) and separated on a C18 in-house packed emitter (1.9 μm; 0.075 × 150 mm) over a 55 min linear gradient (5% to 45%B. A: 2% acetonitrile, 0.1% formic acid B: 80% acetonitrile, 0.1% formic acid). The Orbitrap was set to analyse the survey scans (m/z 350 to 1,600) at 60,000 resolution and the top 10 ions in each duty cycle were selected for MS/MS in the LTQ linear ion trap with collision-induced dissociation (CID) (normalised collision energy (NCE) 36%). The data was searched against the *Mus musculus* Uniprot database (26/05/2015 release; 50,807 entries) using Mascot (2.4.1). Scaffold (4.4.3) was used to validate MS/MS based peptide and protein identifications. Peptide identifications were accepted if they could be established at greater than 95.0% probability as specified by the Peptide Prophet algorithm, resulting in a peptide false discovery rate (FDR) of 0.78% [39]. Protein identifications further required least 2 unique peptides.

For analysis of STBD1 sites phosphorylated *in vivo*, dried peptides were dissolved in 3% acetonitrile/ 0.1% formic acid. RPLC-MS/MS analysis was performed on an LTQ-Orbitrap Velos coupled to a Proxeon Easy-LC using the same chromatography as described above. The Orbitrap was set to analyse the survey scans (m/z 320 to 1,600) at 30,000 resolution and the top 10 ions in each duty cycle were selected for MS/MS in the LTQ linear ion trap with collision-induced dissociation (CID) (NCE 36%; multistage activation was enabled). The data was searched against the *Homo sapiens* Uniprot database (20/12/2012 release; 148,212 entries) using Mascot (2.4.1). All Mascot result files were loaded into Scaffold (4.4.3). Peptide and protein thresholds were set to 95.0% and mascot peptide ion scores were required to be greater than 30, resulting in a peptide FDR of 0.36%. A minimum of 2 unique peptides were required to report protein identification.
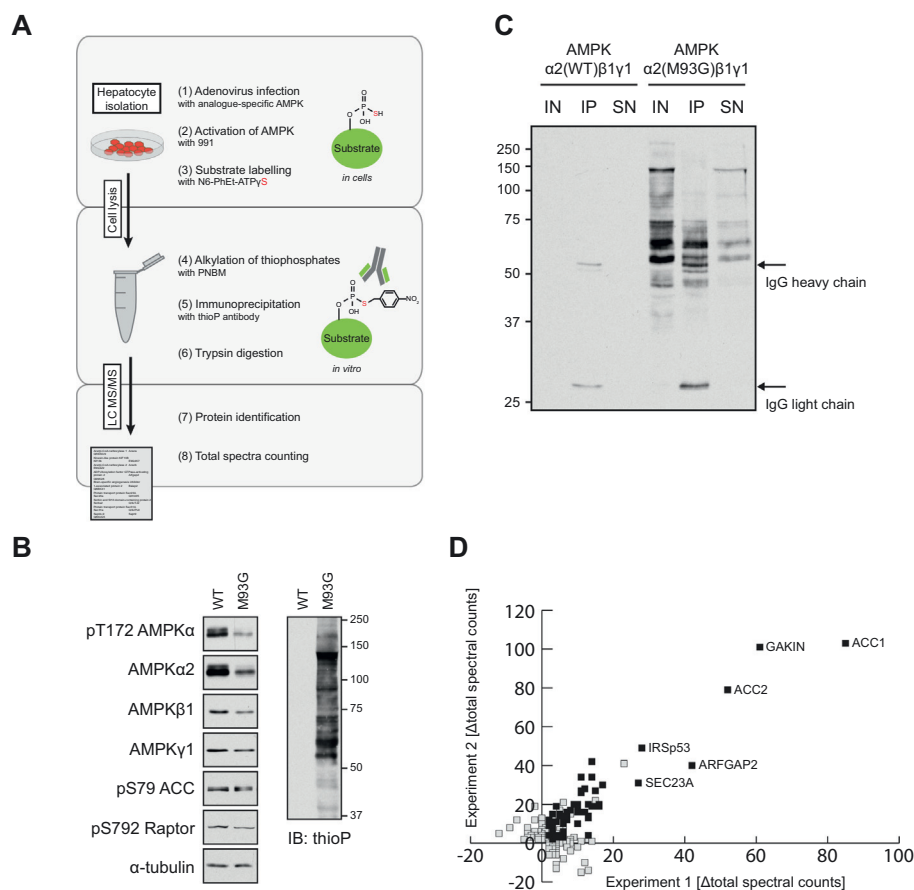
Fig. 1. Chemical genetic screen to identify AMPK substrates. (A) Schematic representation of the workflow used to identify targets of AMPKα2. Primary hepatocytes are isolated from C57BL/6N mice and cultured as described in Materials and methods. The hepatocytes were transduced with adenovirus encoding AMPKβ1, AMPKγ1 and either AMPKα2 WT or M93G (ATP-analogue specific) mutant. The cells were chemically permeabilised and incubated with ATP-analogue (in the presence of 30 μM 991) prior to lysis. Labelled protein were specifically alkylated before immunoprecipitation and then processed for in-gel tryptic digestion and tandem mass spectrometry analysis. (B) Lysates from AMPK-expressing hepatocytes labelled with N⁶-PhEt-ATPγS were separated by SDS-PAGE and immunoblotted with the indicated antibodies (left panel). Lysates alkylated with PNBM were also separated by SDS-PAGE and immunoblotted with the thioP antibody (right panel). (C) 200 μg of alkylated lysates from Fig. 1B (right panel) were immunoprecipitated using the thioP antibody coupled to NHS-activated Sepharose resin. Immunoblotting was performed using the thioP antibody. IN (input): 20 μg alkylated sample, IP: immunoprecipitate, SN (supernatant): 10% of the depleted lysate after IP. (D) The difference in total spectral count between M93G and WT samples was plotted for the first replicate (x-axis) and the second replicate of the experiment (y-axis). Across both independent biological replicates, 272 proteins were identified as positive hits in at least one experiment (open boxes), of which 65 were common to both experiments (filled boxes). The protein names of the top hits are indicated next to their respective data point.

3. Results

3.1. Chemical genetic screen for identification of AMPK substrates in primary mouse hepatocytes

We performed a chemical genetic screen in primary mouse hepatocytes to identify novel AMPK substrates following the work flow illustrated in Fig. 1A. The chemical genetic technology was originally developed based on the evidence that the ATP-binding pocket of protein kinases contains a conserved gatekeeper residue in close contact with the N6 position of the adenine ring of ATP. Replacement of this residue with a smaller amino acid (typically glycine) enables the gatekeeper mutant protein kinase to utilise ATP analogues containing bulky groups at the N6 position [40]. In contrast, the bulky ATP analogues are poor substrates for wild-type (WT) kinases due to the steric hindrance of the gatekeeper residue. N6-modified ATPγS nucleotides are also accepted by the ATP-analogue specific kinase, and the transferred thiophosphate can be alkylated and recognised by a specific monoclonal antibody (Fig. 1A) [40]. This chemical genetic approach allows specific labelling of direct substrates of a protein kinase in cells. A previous study has already identified and confirmed methionine 93 as the gatekeeper residue of AMPKα2 and demonstrated that substitution of methionine 93 to glycine (M93G) transformed the WT into an ATP-analogue specific (AS) form [20].

We transduced mouse primary hepatocytes with adenoviral vector encoding catalytic AMPKα2 WT or M93G mutant in combination with other vectors encoding regulatory AMPKβ1 and AMPKγ1 subunits. We noticed that even though AMPKα2 WT and M93G were transduced at equal MOI, expression of AMPKα2 M93G was markedly lower compared to WT (Fig. 1B, left panel). This was consistently observed across multiple experiments (data not shown), however whether it was due to instability of the M93G mutant or another mechanism is unknown. We

estimate that levels of catalytic α2 subunit expression achieved in WT−/M93G-infected cells are ~10–20-fold higher than endogenous α2 protein expression (data not shown). Coincidentally, the AMPKβ1 and γ1 subunits were also expressed at modestly lower levels when co-transduced with the M93G mutant (Fig. 1B, left panel). Following the adenoviral transduction, hepatocytes were chemically permeabilised and incubated with ATPγS analogue for 20 min in the presence of the specific and potent AMPK activator 991, a small-molecule benzimidazole derivative [41,42]. After alkylation and buffer exchange (as described in Materials and methods), direct immunoblotting of the ATPγS analogue-treated lysates with an anti-thiophosphate-ester (thioP) antibody resulted in a robust and specific labelling of thio-phosphorylated proteins in the AMPKα2 M93G, but not WT-expressing cells- (Fig. 1B), as previously reported [20]. Immunoprecipitation of the labelled lysates with the thioP antibody coupled to NHS-activated Sepharose resin confirmed efficient isolation of the thio-phosphorylated proteins (Fig. 1C). It can be noted that the coupling of the thioP antibody to the resin for immunoprecipitation was also efficient, as only a small amount of IgG heavy and light chains (which react with the secondary antibody) was detected. In order to identify AMPKα2 M93G-mediated thio-phosphorylated proteins by mass spectrometry (MS), we used 2 mg of alkylated lysates from the experiments shown in Fig. 1B (right panel). The lysates were subjected to immunoprecipitation with the thioP antibody or rabbit IgG and the immunoprecipitates were processed for MS analysis as described in the Materials and methods. Extracted peptides analysed by LC-MS/MS were searched against the mouse UniPROT database and the amount of protein detected was quantified by total spectral counting. We performed two independent experiments in which 917 protein clusters were identified with a minimum of two peptides (protein and peptide threshold at 95%). Criteria for positive hits were defined as being either unique to the M93G-transduced sample or at least two-fold enriched in the M93G-

Table 1

The 65 putative AMPK targets that were identified in both experiments. ACC: UniProtKB accession number. T1 and T2: Difference in total spectral counts between the M93G and WT samples for biological replicates 1 and 2, with * indicating that the total spectral count of the WT sample was not zero. Known: Indicates whether the protein has previously been described as an AMPK substrate (with reference).

ACC	Protein name	Representative/proposed function	T1	T2	Known
Q5SWU9	Acetyl-CoA carboxylase 1 (ACC1)	Catalyzes the carboxylation of acetyl-CoA to malonyl-CoA, regulating fatty acid synthesis.	85*	103*	YES [85]
E9Q4K7	Kinesin family member 13B (KIF13B, GAKIN)	Reorganization of cortical cytoskeleton.	61	101	NO
E9Q4Z2	Acetyl-CoA carboxylase 2 (ACC2)	Catalyzes the carboxylation of acetyl-CoA to malonyl-CoA, regulating fatty acid oxidation.	52*	79	YES [86]
Q99K28	ADP-ribosylation factor GTPase-activating protein 2 (ARFGAP2)	Implicated in coatomer-mediated protein transport between Golgi complex and ER.	42	40	NO
Q8BKX1	Brain-specific angiogenesis inhibitor 1-associated protein 2 (BAIAP2, IRSp53)	Reorganization of actin cytoskeleton, involved in lamellipodia and filopodia formation in motile cells.	28	49	YES [20,21]
Q01405	Transport protein Sec23A	Component of the COPII coat, that covers vesicle transport from the ER to the Golgi apparatus.	27*	31*	NO
Q3UTJ2	Sorbin and SH3 domain-containing protein 2 (SORBS2, ArgBP2)	Plays a role in the assembling of signaling complexes in stress fibers.	14	42	NO
Q3UPL0	Transport Protein Sec31A	Component of the outer layer of the coat protein complex II, involved in vesicle budding from the ER.	14*	34	NO
Q80UG5	Septin 9	May play a role in cytokinesis and cell cycle control.	17*	30	NO
Q3UMF0	Cordon-bleu protein-like 1	Unknown function.	11*	34	YES [14]
Q9QYG0	N-Myc Downstream-Regulated Gene 2 Protein (NDRG2)	Contributes to the regulation of the Wnt signaling pathway.	15	27	NO
Q8VCF0	Mitochondrial antiviral-signaling protein (MAVS)	Required for innate immune defense against viruses.	12	28	NO
Q01279	Epidermal growth factor receptor (EGFR)	Receptor tyrosine kinase initiating several signal transduction cascades such as MAPK, Akt and JNK pathways.	11	27	NO
P30999	Catenin delta-1 (p120 catenin)	Regulates cell adhesion by association with cadherins.	11	26	YES [21,49]
O88343	Electrogenic sodium bicarbonate cotransporter 1 (NBCe1, SLC4A4)	May regulate bicarbonate influx/efflux at the basolateral membrane of cells and regulate intracellular pH.	16	20	YES [14]
Q9DBJ3	Brain-specific angiogenesis inhibitor 1-associated protein 2-like protein 1 (BAIAP2L1, IRTKS)	Plays a role in actin cytoskeleton reorganization, involved in the formation of clusters of actin bundles.	16	19	YES [20,21]
O55131	Septin 7	Required for normal organization of the actin cytoskeleton and mitosis.	15	19	NO
P70266	6-phosphofructo-2-kinase/fructose-2,6-bisphosphatase 1 (PFK/FBPase 1)	Synthesis and degradation of fructose 2,6-bisphosphate.	13	20	NO
Q61768	Kinesin-1 heavy chain (KIF5B)	Microtubule-dependent motor required for normal distribution of mitochondria and lysosomes.	14*	19	NO
Q8R1S4	Metastasis suppressor protein 1 (MTSS1)	Inhibits the nucleation of actin filaments in vitro.	10	20	YES [14]
Q9ET54	Palladin	Cytoskeletal protein required for organization of normal actin cytoskeleton.	9	20	NO
Q8BUV3	Gephyrin	Microtubule-associated protein involved in membrane protein-cytoskeleton interactions.	12*	16*	YES [20,21]
Q8C7E7	Starch-binding domain-containing protein 1 (STBD1)	Cargo receptor for glycogen, resulting in the transport of glycogen to lysosomes.	13	14	NO
Q99JX3	Golgi reassembly-stacking protein 2 (GRS2, GRASP55)	Plays a role in Golgi cisternae assembly, membrane stacking and reforming after mitotic breakdown.	11	16	NO
Q99MI1	ELKS/Rab6-interacting/CAST family member 1 (ERC1)	Regulatory subunit of IKK complex. May be involved in Rab-6 regulated endosomes to Golgi transport.	10	17	NO
Q8BRK8	5'-AMP-activated protein kinase catalytic subunit alpha-2 (AMPKα2)	Catalytic subunit of AMPK, an energy sensor protein kinase regulating cellular energy metabolism.	10	16	YES
Q62261	Spectrin beta chain, non-erythrocytic 1 (SPTBN1)	Component of spectrin, an actin crosslinking and molecular scaffold protein that links the plasma membrane to the actin cytoskeleton.	13*	13	NO
P26231	Catenin alpha-1 (α-E-Catenin)	Regulates cell adhesion by association with cadherins.	8	17	NO
Q9DBR7	Protein phosphatase 1 regulatory subunit 12A (PPP1R12A, MYPT1)	Part of myosin phosphatase, regulates actin to myosin interactions.	7	16	YES [20,21]
E9Q9M1	Cytosolic purine 5'-nucleotidase (NT5C2)	May play a role in the maintenance of a constant composition of intracellular purine/pyrimidine nucleotides.	4	19	NO
Q6PA06	Atlastin-2	Functions in endoplasmic reticulum tubular network biogenesis.	7	15	NO
Q9JMH9	Unconventional myosin-XVIIIa (MYO18A)	Links Golgi and cytoskeleton, influencing Golgi membrane trafficking.	7	13	NO
Q62QB6	Diphosphoinositol Pentakisphosphate Kinase 2 (PPIP5K2, VIP2)	Synthesizes high-energy inositol pyrophosphates, which act as signaling molecules that regulate cellular homeostasis and other processes.	6	14	NO
P42208	Septin 2 (NEDD5)	Required for normal organization of the actin cytoskeleton and mitosis.	5	15	NO
P97742	Carnitine O-palmitoyltransferase 1, liver isoform (CPT1a)	Key enzyme in the carnitine-dependent transport of long-chain fatty acids into mitochondria and their subsequent beta-oxidation.	10*	10*	NO
Q9WUK2	Eukaryotic translation initiation factor 4H (EIF4H)	Stimulates the RNA helicase activity of EIF4A in the translation initiation complex.	5	14	NO
Q8BFY9	Transportin-1 (TNPO1)	Functions in nuclear protein import as nuclear transport receptor for nuclear localization signals (NLS).	7*	12*	YES [20,21]
Q3U2P1	Transport protein Sec24A	Component of the COPII coat, that covers vesicle transport from the ER to the Golgi apparatus.	5*	14	YES [20,21]
Q3UMT1	Protein phosphatase 1 regulatory subunit 12C (PPP1R12C, MBS85)	Part of myosin phosphatase, regulates actin cytoskeleton assembly.	3	15	YES [20]
Q6NXL1	Transport Protein Sec24D	Component of the COPII coat, that covers vesicle transport from the ER to the Golgi apparatus.	6*	12	NO
Q68FG2	Spectrin Beta, non-erythrocytic 2 (SPTBN2)	Regulates the glutamate signaling pathway by stabilizing the glutamate transporter EAAT4 at the surface of the plasma membrane.	13*	4	NO
Q9D1M0	SEC13-Related Protein	Involved in biogenesis of COPII-coated vesicles. Component of GATOR complexes influencing mTORC1 signaling.	6	10	NO
Q02248	Catenin beta-1 (β-Catenin)	Key component of WNT signaling, transcriptional coactivator. Involved in cell adhesion.	4	11	NO
Q62433	N-Myc Downstream-Regulated Gene 1 Protein (NDRG1)	Involved in stress and hormone response, cell growth and differentiation.	2	12	NO
Q9R078	5'-AMP-activated protein kinase subunit beta-1 (AMPKβ1)	Non-catalytic subunit of AMPK, an energy sensor protein kinase regulating cellular energy metabolism.	3	11*	YES
Q9DBS5	Kinesin light chain 4 (KLC4)	Component of kinesin, plays a role in organelle transport.	6	6	NO
Q8CIN4	Serine/threonine-protein kinase PAK 2	Plays a role in a variety of different signaling pathways, including cell survival and cell growth.	3	8	YES [20]
Q3UMY5	Echinoderm microtubule-associated protein-like 4 (EML4)	May modify assembly dynamics of microtubules, making them slightly longer, but more dynamic.	2	9	NO

(continued on next page)

Table 1 (*continued*)

ACC	Protein name	Representative/proposed function	T1	T2	Known
P70302	Stromal interaction molecule 1 (STIM1)	Ca2+ sensor, plays a role in mediating store-operated Ca2+ entry.	3	8	YES [49]
Q3UW64	Bifunctional UDP-N-acetylglucosamine 2-epimerase/N-acetylmannosamine kinase (GNE)	Rate-limiting enzyme in the sialic acid biosynthetic pathway which plays a role in cell adhesion, signal transduction and other processes.	6*	4	NO
Q6PAR5	GTPase-activating protein and VPS9 domain-containing protein 1 (Gapex-5)	Participates in various processes such as endocytosis, insulin receptor internalization or GLUT4 trafficking.	6*	4	YES [14]
Q04207	Transcription factor p65	Part of the NF-κB pathway, involved in inflammation, cell growth and many other cellular processes.	3	6	NO
D3YXZ3	Kinesin light chain 2 (KLC2)	Component of kinesin, plays a role in organelle transport.	5	4	NO
Q9CZW5	Mitochondrial import receptor subunit TOM70	Receptor that accelerates the import of all mitochondrial precursor proteins.	6	3	NO
Q8BP47	Asparagine-tRNA ligase, cytoplasmic (AsnRS)	Charges tRNA with asparagine.	6	3	NO
Q9D662	Transport protein Sec23B	Component of the COPII coat, that covers vesicle transport from the ER to the Golgi apparatus.	5*	4*	NO
Q6NZC7	SEC23-interacting protein	Plays a role in the organization of endoplasmic reticulum exit sites.	3	5	NO
Q9CY27	Very-long-chain enoyl-CoA reductase (TER)	Catalyzes the last of the four reactions of the long-chain fatty acids elongation cycle.	5	3	NO
Q8R3V5	Endophilin-B2	May play a role in inner mitochondrial membrane degradation or endosome maturation.	4	4	NO
P28660	Nck-associated protein 1 (NAP1, NCKAP1)	Part of the WAVE complex that regulates lamellipodia formation through actin filament reorganization.	3*	5	YES [14,20]
A2AE27	AMP deaminase 2	Catalyzes the deamination of AMP to IMP and plays an important role in the purine nucleotide cycle.	4	3	NO
Q9CVB6	Actin-related protein 2/3 complex subunit 2 (ARPC2, p34-ARC)	Functions as actin-binding component of Arp2/3 complex involved in regulation of actin polymerization.	3	3	NO
Q07113	Cation-independent mannose-6-phosphate receptor (CI-MPR, IGF2R)	Transport of phosphorylated lysosomal enzymes from the Golgi complex and the cell surface to lysosomes.	2	4	YES [20]
Q9CY50	Translocon-associated protein subunit alpha (TRAPα, SSR1)	Part of a complex whose function is to bind calcium to the ER membrane and thereby regulate the retention of ER resident proteins.	3	3*	NO
P46061	Ran GTPase-activating protein 1 (RanGAP1)	Associates with the nuclear pore complex and participates in the regulation of nuclear transport.	3	2	NO

transduced samples as compared to the WT-transduced sample. Across biological repeats, 272 proteins were identified as positive hits, of which 65 were common to both biological replicates (Table 1). For those proteins, there was a good correlation (R^2 of 0.85) of total spectra counts detected between the two runs, demonstrating that the current experimental approach had high reproducibility (Fig. 1D). Amongst the 65 proteins identified were well established (ACC1, ACC2) or recently reported (MBS85 (also known as PPP1R12C), PAK2 and IRSp53 (also known as BAIAP2)) [20] substrates of AMPK. Based on our primary interest in the role of AMPK in nutrient transport [2,10,43] and glycogen metabolism [44–46], we decided to focus on Gapex-5 (which has been proposed to play a role in vesicle trafficking) and STBD1 (which is known as starch/glycogen binding protein).

3.2. Identification and validation of Gapex-5 and STBD1 as novel substrates of AMPK

In the experimental approach used in this study, it was not possible to directly determine the specific site of thio-phosphorylation in the protein/peptides. Using the MS data from our previous study [14], we identified a phospho-peptide (SR*SSDIVSSVR, the prefix * denotes the phosphorylated residue) which was uniquely present in samples from hepatocytes treated with a combination of two AMPK activators (AICAR and A769662) [36,47], but not in samples from vehicle-treated control or AMPK-deficient hepatocytes. This phospho-peptide is proteotypic to Gapex-5, and the phosphorylated residue corresponds to Ser902 (of mouse and also human Gapex-5). Ser902 Gapex-5 is well conserved across the species examined and falls optimally into the AMPK phosphorylation motif [21] (Fig. 2A). In order to validate AMPK-mediated phosphorylation of Gapex-5, we cloned human Gapex-5 and custom-generated a phosphosite-specific antibody for detection of Ser902 (p-Ser902 as described in Materials and methods). We transfected COS-1 cells with FLAG-tagged WT or non-phosphorylatable S902A mutant of Gapex-5 and treated the cells with either 991 or vehicle for 30 min followed by immunoblot analysis (Fig. 2B). As anticipated, 991 treatment resulted in a robust increase in phosphorylation of AMPK and its established *bona fide* substrate ACC. We observed that 991 increased Gapex-5 Ser902 phosphorylation in WT, but not in S902A mutant AMPK, confirming the MS result and also specificity of the p-Ser902 antibody (Fig. 2B). We further verified specific phosphorylation of Gapex-5 Ser902 using the AMPK phosphorylation motif antibody. The expected molecular weight is 164 kDa and we observed that the major band for FLAG-Gapex-5 was detected just below the 250 kDa marker (when proteins were resolved in 8% tris-glycine SDS-PAGE). Upon longer exposure of the immunoblots, an additional band was detected around 150 kDa. This band could represent a degradation product (C-terminal truncated) of the full-length (N-terminal FLAG-tagged Gapex-5) protein (Fig. 2B). We then sought to investigate whether endogenous Gapex-5 is regulated by AMPK in intact cells. We first assessed Gapex-5 expression in a panel of mouse tissues using two different antibodies; one raised against the N-terminus and the other against an internal sequence of human Gapex-5. Indeed, Gapex-5 was detectable in most mouse tissues analysed (including liver), but not detectable in kidney (Fig. 2C). Consistent with the results obtained with recombinant FLAG-Gapex-5 (Fig. 2B), we observed that endogenous Gapex-5 also runs just below the 250 kDa marker (Fig. 2C), and the specificity of the antibody was also confirmed on tissues from Gapex-5 knockout zebrafish that we generated (Supplemental Fig. S3E). We next wanted to validate AMPK-mediated phosphorylation of endogenous Gapex-5 in intact hepatocytes. In the AML12 mouse hepatocyte cell line, Gapex-5 was phosphorylated on Ser902 upon treatment with AICAR and A769662, which was detected using either the AMPK phospho-motif antibody or the phosphosite-specific antibody for Ser902 following immunoprecipitation with a total Gapex-5 antibody (Fig. 2D). We next treated hepatocytes, isolated from hepatic AMPKα1/α2 double knockout (DKO) and floxed control mice, with AICAR and A769662. As shown in Fig. 2E,
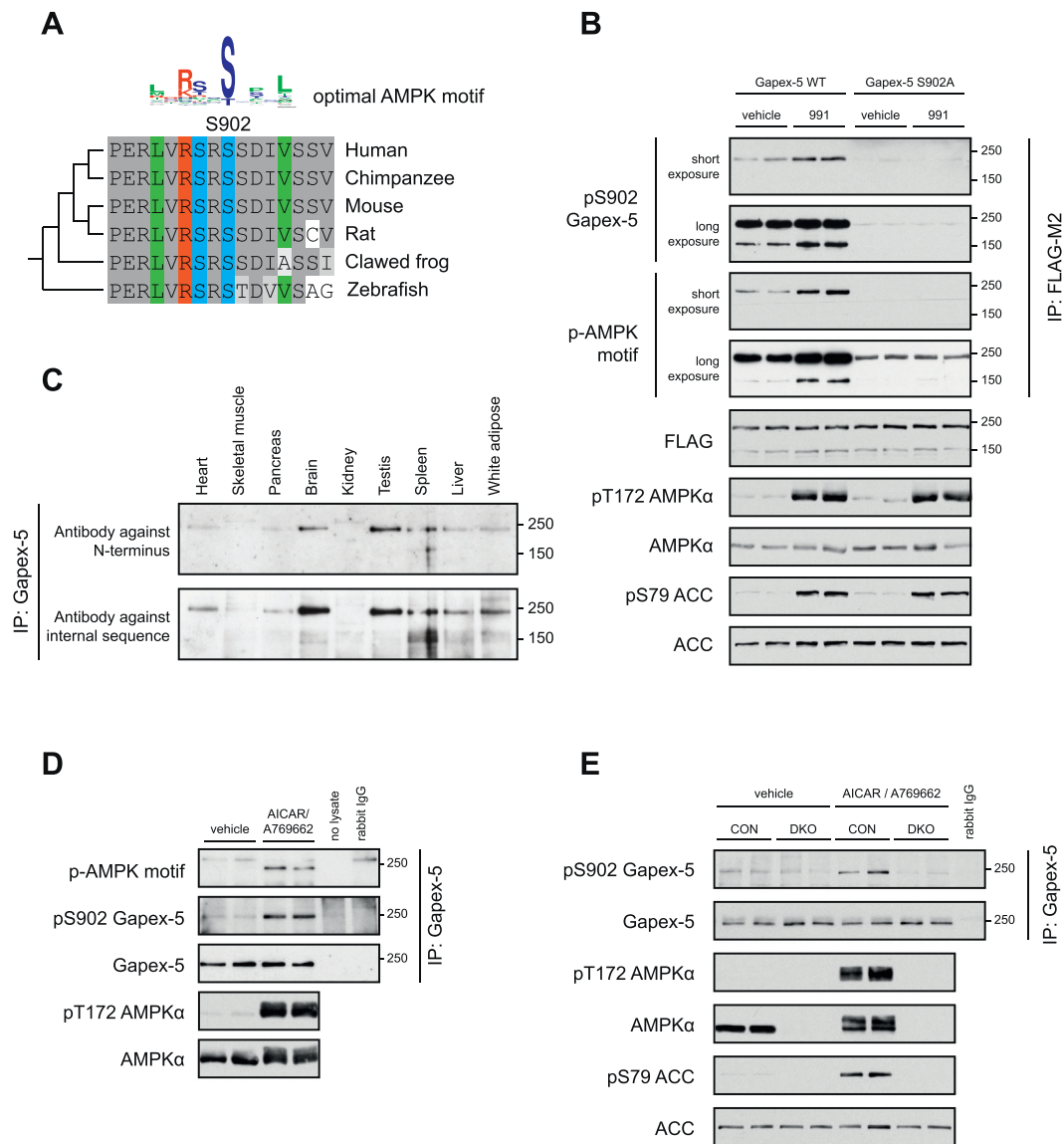
Fig. 2. Biochemical characterisation of Gapex-5 as an AMPK substrate. (A) Sequences of Gapex-5 from chimpanzee (Uniprot identifier: K7D792), mouse (Q6PAR5), rat (D3ZBJ3), clawed frog (A2RV61) and zebrafish (E7F237) were aligned to the human sequence (Q14C86) using ClustalW (www.clustal.org). The sequence surrounding Ser902 of human Gapex-5 is shown. The sequence for the optimal AMPK motif was created using WebLogo (weblogo.berkeley.edu) and the sequences surrounding a list of *in vivo* AMPK phosphorylation target sites as compiled by Schaffer et al. [21]. (B) COS-1 cells were transfected with human FLAG-Gapex-5 wildtype (WT) or S902A mutant. Cells were then treated with vehicle (0.1% DMSO) or 10 µM 991 for 30 min. Gapex-5 was immunoprecipitated with FLAG-M2 antibody from 100 µg cell lysates. Western blotting was performed using the immunoprecipitates and input lysates (20 µg) using the indicated antibodies. Immunoblots shown are representative of two independent experiments. (C) Tissue protein extracts were prepared from C57BL/6N mice. Total cell lysates (200 µg) were immunoprecipitated using anti-Gapex-5 antibody (internal sequence) and Protein G Sepharose. Western blotting was performed using two different anti-Gapex-5 antibodies. Immunoblots shown are representative of two independent experiments. (D) AML12 mouse hepatocytes were treated with vehicle or a combination of 1 mM AICAR and 30 µM A769662 for 30 min. Total cell lysates (200 µg) were immunoprecipitated using anti-Gapex 5 (internal sequence) or non-specific control antibody (rabbit IgG) and Protein G Sepharose. Western blotting of the immunoprecipitates and input lysates (20 µg) was performed using the indicated antibodies. Immunoblots shown are representative of two independent experiments. (E) Primary hepatocytes were isolated from AMPKα1/α2 liver-specific double knockout (DKO) and control AMPKα1$^{lox/lox}$α2$^{lox/lox}$ mice (CON). Plated hepatocytes were treated with vehicle or a combination of 0.3 mM AICAR and 10 µM A769662 for 45 min. Total cell lysates (400 µg) were immunoprecipitated using anti-Gapex-5 (internal sequence) or non-specific control antibody (rabbit IgG) and Protein G Sepharose. Western blotting of the immunoprecipitates and input lysates (20 µg) was performed using the indicated antibodies. Immunoblots shown are representative of two independent experiments.

upon treatment with the compounds, Gapex-5 Ser902 phosphorylation was increased in control hepatocytes, but not in AMPK DKO hepatocytes. Taken together, these results demonstrate that Gapex-5 is phosphorylated at Ser902 in hepatocytes in an AMPK-dependent manner, which could likely account for the direct AMPK phosphorylation event identified in our chemical genetic screen.

We next wanted to validate/establish if STBD1 is a novel AMPK substrate. Consistent with the results presented in a previous study

[48], STBD1 is predominantly expressed in liver, skeletal muscle and to a lesser extent in the spleen of the mouse tissues analysed (Fig. 3A). Next, we wanted to identify specific site(s) on STBD1 phosphorylated by AMPK. Inspection of the STBD1 protein sequence, both manually and also using AMPK motif scan by Scansite (http://scansite.mit.edu/), revealed that several sites conform to the AMPK phosphorylation motif to varying degrees. However, contrary to our expectation, immunoblotting of the 991-treated cell lysates with the phospho-AMPK
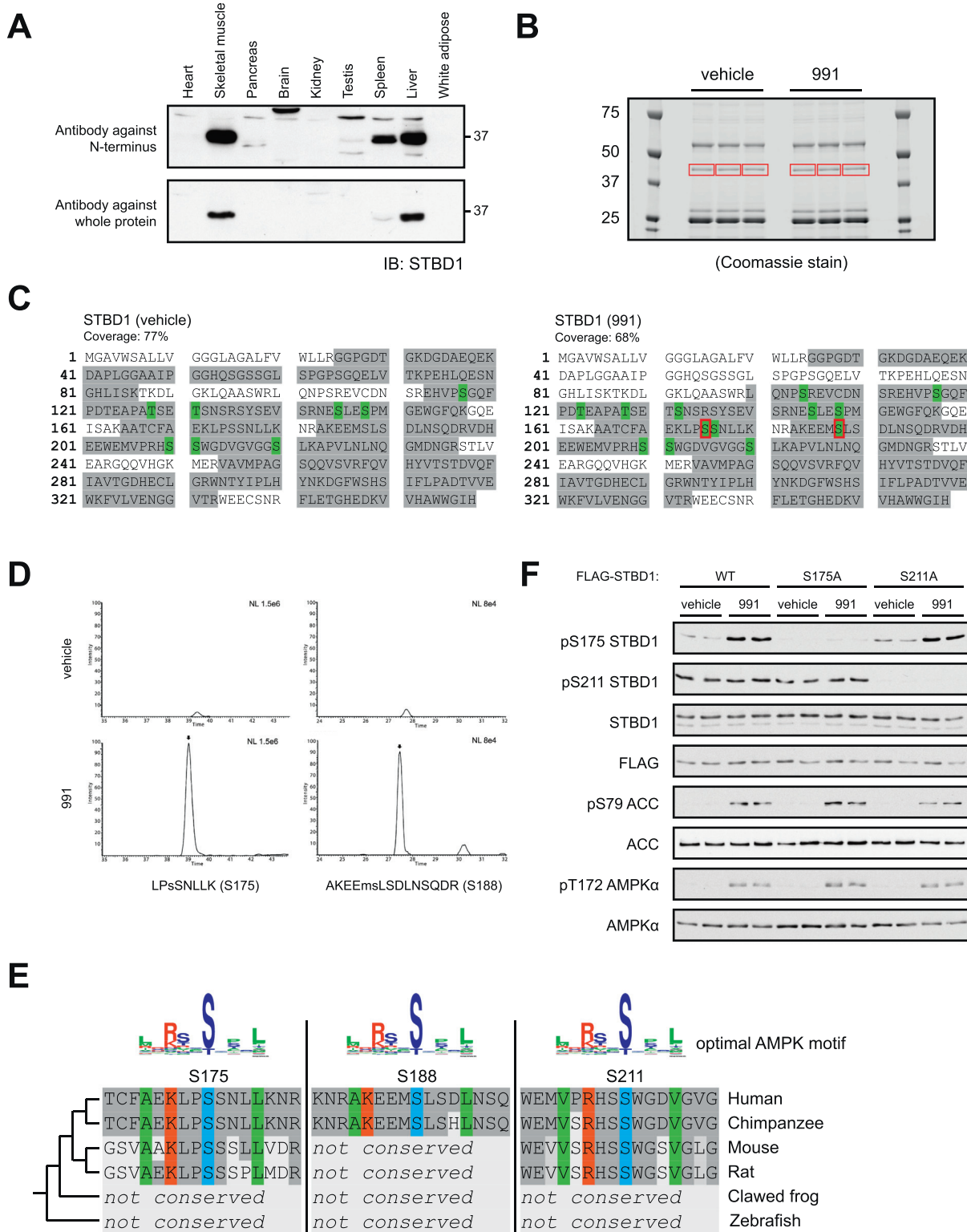
(caption on next page)

motif antibody failed to detect a signal on ectopically expressed FLAG-STBD1 (data not shown). We therefore decided to perform unbiased phospho-peptide mapping by MS. FLAG-STBD1 was transiently over-expressed in COS-1 cells and they were treated with vehicle or 991 (30 μM) for 1 h. Recombinant STBD1 was affinity purified with a FLAG antibody, digested in-gel with trypsin and the resulting peptides were subjected to MS analysis (Fig. 3B). The MS/MS analysis resulted in

peptide coverage of STBD1 ranging from 68% to 77% and revealed multiple phosphorylated residues (Fig. 3C). Of those residues, Ser175 and Ser188 were consistently identified phosphorylation sites in all three replicates under the 991-treated conditions. We also inspected the extracted ion chromatograms (XIC) corresponding to those residues (LP*SSNLLK for Ser175 and AKEEM*SLSDLNSQDR for Ser188). Indeed, the XIC clearly confirmed the presence of the phosphorylated phospho-

Fig. 3. Biochemical characterisation of STBD1 as an AMPK substrate. (A) Tissue extracts were prepared from C57BL/6N mice. Western blotting using 20 μg lysates was performed using two different anti-STBD1 antibodies. Immunoblots are representative of 3 independent experiments. (B) COS-1 cells were transfected with human FLAG-STBD1. Cells were then serum-starved for 4 h before treatment with vehicle (0.1% DMSO) or 30 μM 991 for 1 h. FLAG-STBD1 was affinity purified with FLAG-M2 resin from 500 μg cell lysates, separated by SDS-PAGE and the gel was stained using Coomassie dye. (C, D) Gel pieces containing STBD1 from Fig. 3B (red boxes) were excised for further processing (trypsin digestion and tandem mass spectrometry analysis). (C) Sequence coverage (merged results for 3 samples) for samples from vehicle-treated (left panel) and 991-treated cells (right panel) are shown (grey shading), along with phosphorylated residues (green shading). Residues phosphorylated uniquely in samples from 991-treated cells and that were present in all 3 samples are marked with a red box. (D) Extracted ion chromatograms are shown for two phospho-peptides, LPsSNLLK and AKEEmsLSDLNSQDR (lowercase denotes phosphorylated serine or oxidized methionine residue). For each phospho-peptide, ion intensities were normalised to the same scale between vehicle- and 991-treated samples. Peptides were identified by MS/MS spectra exclusively after 991 treatment and recorded at the time indicted with the arrow. NL: normalization level. (E) Sequences of STBD1 from chimpanzee (Uniprot identifier: H2QPQ7), mouse (Q8C7E7), rat (Q5FVN1), clawed frog (A9JTP4) and zebrafish (E7FH49) were aligned to the human sequence (O95210) using ClustalW (www.clustal.org). The regions around Ser175, Ser188 and Ser211 of human STDB1 are shown. The sequence for the optimal AMPK motif was created using WebLogo (weblogo.berkeley.edu) and the *in vivo* sequences of known AMPK substrates according to Schaffer et al. [21]. (F) COS-1 cells were transfected with human FLAG-STBD1 wild-type, Ser175Ala or Ser211Ala mutant. Cells were then treated with vehicle (0.1% DMSO) or 30 μM 991 for 30 min. Lysates (10 μg) were separated by SDS-PAGE and immunoblotted using the antibodies as indicated. Immunoblots are representative of 2 independent experiments.

peptide only in 991-treated samples (Fig. 3D). Both of the identified 991-regulated sites fit relatively well with the broadly defined AMPK phosphorylation motif [12], with hydrophobic alanine and leucine residues at the −5 and +4 positions, with respect to the phosphorylation site, and a basic lysine residue at the −3 or −4 position (Fig. 3E). In addition to the 991-regulated phosphorylation sites identified by MS, during manual inspection of the STBD1 sequence, we noticed Ser211 and its surrounding sequence conforming to the optimal AMPK motif (Fig. 3E). We then generated phosphosite-specific antibodies for the well-conserved (across mammals) residues (Ser175 and Ser211) but not the less conserved Ser188 site (Fig. 3E). We ectopically overexpressed (FLAG-tagged) WT or non-phosphorylatable (Ser175Ala or Ser211Ala) STBD1 in COS-1 cells and the cells were treated with 991. This treatment comparably promoted phosphorylation of AMPK and ACC, while it robustly stimulated phosphorylation of WT FLAG-STBD1 on Ser175, but not the Ser175Ala mutant (Fig. 3F). In contrast, while Ser211 phosphorylation was readily detected under basal (vehicle-treated) condition, it was not increased with 991 treatment under the condition tested.

We next investigated Ser175 phosphorylation of endogenous STBD1 upon AMPK activation in mouse primary hepatocytes. Treatment with AICAR robustly increased pSer175-STBD1 in a dose-dependent manner and followed the increase of AMPK phosphorylation on Thr172 and of the *bona fide* AMPK substrate Raptor on Ser792 (Fig. 4A and B). Furthermore, increased pSer175-STBD1 was also observed upon treatment of primary mouse hepatoctyes with 991 (Supplemental Fig. S4A and S4B). In order to establish AMPK dependence of Ser175-STBD1 phosphorylation, we treated hepatocytes, isolated from hepatic AMPK double KO and control mice, with single (10 μM 991) or dual (0.3 mM AICAR + 10 μM A769662) AMPK activator treatment (Fig. 4C). Consistent with our previous observations [36,47], dual treatment (AICAR/A769662) caused a profoundly higher phosphorylation of AMPK and its known substrate Raptor compared to single treatment. Notably, the dual treatment markedly increased Ser175 phosphorylation of STBD1, which was accompanied by an upward shift of the immune-reactive band, possibly due to additional phosphorylation events beside Ser175 on STBD1. Under these conditions, the total STBD1 antibody used was unable to detect the total STBD1 protein, possibly due to significant modulation of the epitope sequence *via* multiple phosphorylation resulting in insufficient recognition by the antibody (Fig. 4C). Furthermore, we confirmed that Ser175 phosphorylation in vehicle- and activator-stimulated conditions was totally AMPK-dependent, as the phosphorylation signals were abolished in the AMPK DKO hepatocytes (Fig. 4C). To investigate STBD1 phosphorylation in skeletal muscle, extensor digitorum longus (EDL) muscle was isolated from wild-type mice and mice with muscle-specific overexpression of kinase-dead AMPK (AMPK-KD) [35] and incubated with vehicle or 4 mM AICAR. As shown in Fig. 4D, AICAR treatment increased AMPK (Thr172) and ACC (Ser79) phosphorylation in muscles from wild-type mice but not in muscles isolated from AMPK-KD mice. The antibody raised against

pSer175-STBD1 also shows a non-specific immune-reactive band just above 37 kDa in skeletal muscle, nevertheless the antibody detected increased Ser175-STBD1 phosphorylation (just below 37 kDa) upon AICAR treatment of muscle from wild-type mice, but this effect was lost in EDL muscle isolated from AMPK kinase-dead mice (Fig. 4D). In summary, these results establish STBD1 Ser175 as a novel AMPK target site both in liver as well as in skeletal muscle.

4. Discussion

To better understand physiological consequences of AMPK activation, identifying the downstream effectors in a cell- and activator-specific context is essential. With previous screens for cellular AMPK targets having been performed in immortalised cell lines such as HEK293T [20], U2OS [21] or L6 myotubes [49], we have focused on identifying AMPK targets in primary hepatocytes, such as to account for a cell- and tissue-specific role of AMPK. To do that, we have recently established an MS-based analysis of proteins isolated from mouse hepatocyte extracts using a phospho-AMPK substrate motif antibody [14]. Even though the motif affinity proteomics approach is simple and valid in identifying cellular AMPK targets, it has a limitation in that it has a bias towards proteins containing the strict AMPK consensus motif with a leucine at the −5 and an arginine at the −3 position [14]. To overcome this limitation and implement a complementary approach to more comprehensively identify AMPK-dependent cellular targets, we have undertaken a chemical genetic approach using ATP-analogue specific AMPK, which is expected to have the same substrate specificity as compared to endogenous AMPK [20]. We report 65 potential direct targets of AMPK in primary hepatocytes, amongst them well established (ACC1, ACC2) or recently reported (MBS85 (also known as PPP1R12C), PAK2 and IRSp53 (also known as BAIAP2)) [20] substrates of AMPK. Based on literature analysis, the identified proteins are involved in lipid, carbohydrate and nucleotide metabolism, as well as immune response, cell adhesion, cytoskeleton organisation, protein trafficking and other cellular processes as summarised in Table 1. We also compared the current hits with the ones obtained through the aforementioned motif proteomics approach, in which 57 proteins were described as AMPK-dependent phosphorylation targets [14]. Although both studies were performed in the same cellular system, only 6 proteins (ACC1, Gapex-5, COBLL1, NBCe1, MTSS1 and NAP1) were in common between the two studies. The limited overlap can be explained by several reasons: For example, overexpression of ATP-analogue specific AMPK might affect subcellular localisation of the kinase, and introduction of a mutation in the kinase ATP-binding pocket could affect substrate phosphorylation kinetics. Collectively, this suggests that because of biases introduced by the methodology, as well as issues of sensitivity, either method only detects a subset of all AMPK substrates in hepatocytes. This is further corroborated by the fact that ubiquitous *bona fide* substrates such as Raptor and Ulk1 were not identified in our screens.

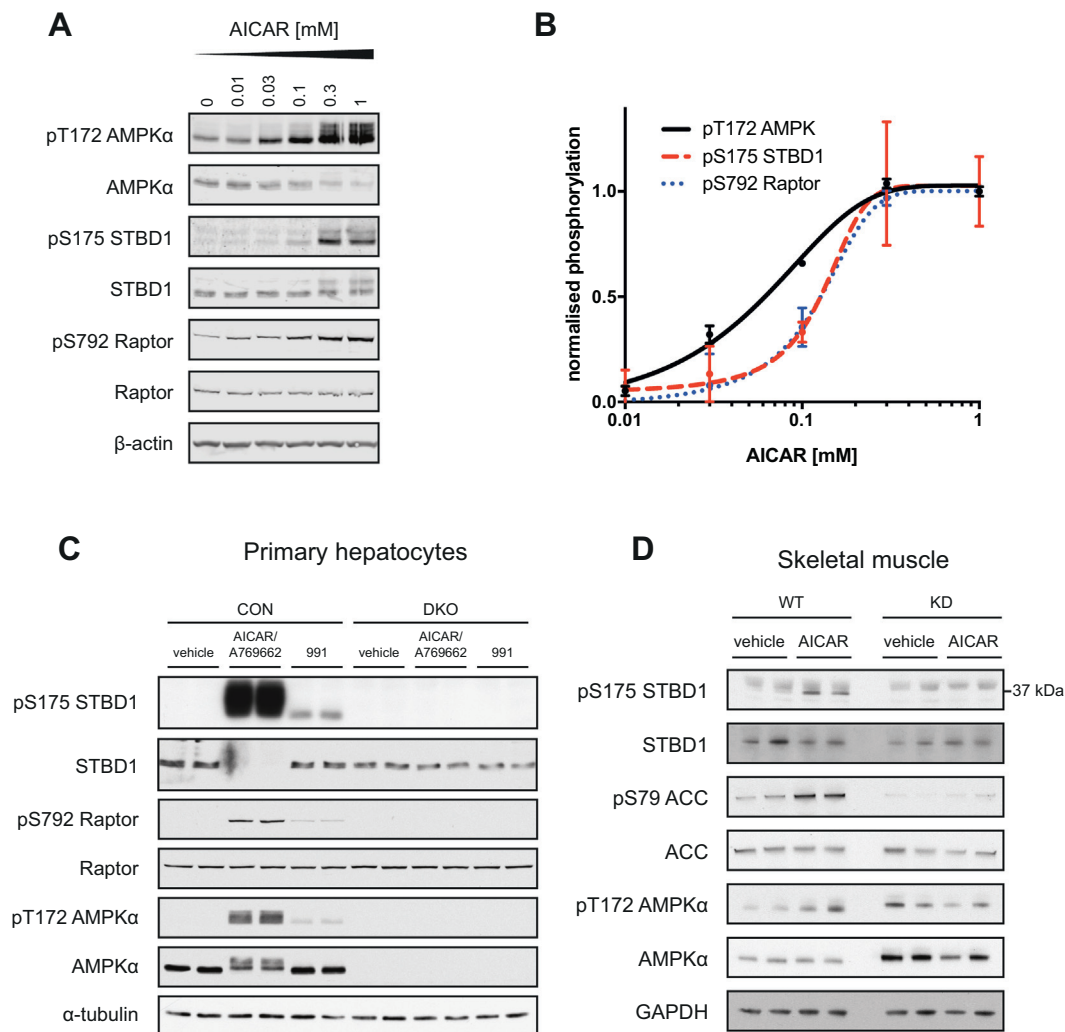AMPK has previously been shown to regulate vesicle trafficking

Fig. 4. Phosphorylation of STBD1 in primary hepatocytes and skeletal muscle. (A,B) Primary hepatocytes were isolated from C57BL/6N mice, and treated with vehicle or AICAR at the indicated concentrations for 1 h. (A) Western blotting was performed using total lysates (20 μg) using the indicated antibodies, and detection was performed with the Odyssey CLx Imaging System (LI-COR Biosciences). Immunoblots are representative of 2 independent experiments. (B) Western blots were quantified using Image Studio v3.1 (LI-COR Biosciences). Phosphorylated protein intensities were normalised to β-actin, and fold increase over vehicle-treated condition is shown as mean ± standard error (n = 2), fitted with a sigmoidal dose-response (variable slope) curve (GraphPad Prism 7). (C) Primary hepatocytes were isolated from AMPKα1/α2 liver-specific double knockout (DKO) and control AMPKα1$^{lox/lox}$α2$^{lox/lox}$ mice (CON). The hepatocytes were treated with vehicle, a combination of 0.3 mM AICAR and 10 μM A769662, or 10 μM 991 for 45 min. Western blotting was performed using total lysates (10 μg) using the indicated antibodies. Immunoblots are representative of 2 independent experiments. (D) EDL muscles from wild-type (WT) mice or mice with muscle-specific overexpression of kinase-dead AMPK (AMPK-KD) were isolated and incubated with vehicle or 4 mM AICAR for 40 min. Muscles were homogenised and protein extracts (20 μg) were analysed by immunoblotting with the indicated antbodies. Representative immunoblots are shown, n = 4.

under certain conditions, notably in the context of CD36-mediated fatty acid uptake [50–53] and GLUT4-mediated glucose uptake [8,54,55] into striated muscle. The latter has furthermore been shown to depend on phosphorylation of the Rab GTPase-activating protein (RabGAP) TBC1D1 on Ser237 by AMPK [10,56–58]. Moreover, AMPK has been implicated in endocytic processes, such as regulation of GLUT1 endocytosis through phosphorylation of TXNIP [59]. Gapex-5 (also known as RAP6, gene name *gapvd1*) was identified as an AMPK substrate in the present study as well as in our AMPK motif screen [14] and we demonstrated AMPK-dependent Gapex-5 phosphorylation on Ser902 in intact primary hepatocytes (Fig. 2). Gapex-5 is an endosomal protein which contains a Ras GTPase-activating protein (RasGAP) domain at the N terminus and a C-terminal Vps9 domain (Supplemental Fig. S3A), the latter serving as a guanine exchange factor (GEF) domain for Rab5 [60]. Gapex-5 has been implicated in both fluid-phase as well as receptor-mediated endocytosis in various cell lines [60–62]. To investigate a potential involvement of AMPK and Gapex-5 in regulation of

endocytosis in hepatocytes, we measured uptake of low-density lipoprotein (LDL) and epidermal growth factor (EGF) into primary mouse hepatocytes. We found that specific AMPK activation with 991 slowed down endosomal trafficking for both LDL and EGF (Supplemental Fig. S1A,B). Whereas Gapex-5 knockdown had no effect on EGF trafficking, it resulted in reduced LDL endocytosis (Supplemental Fig. S1C-E). This is in agreement with the reported function of Gapex-5 as a GEF for Rab5 since uptake of LDL, which is a classical clathrin-dependent endocytosis target, was shown to be largely dependent on Rab5 [63]. EGF on the other hand has been shown to enter the cell through multiple pathways [64,65].

In adipocytes, Gapex-5 has been implicated in regulation of GLUT4 vesicle trafficking [66,67]. Gapex-5 has been proposed to cause intracellular retention of GLUT4 vesicles through activation of Rab31, a Rab5 family member, in the cytosol [67]. Upon insulin stimulation, Gapex-5 was shown to translocate to the plasma membrane, leading to activation of Rab5 [66]. Accordingly, knockdown of Gapex-5 in 3 T3-L1

adipocytes has been shown to reduce insulin-stimulated glucose uptake [66]. To confirm this result, we have knocked down Gapex-5 using three different siRNA in 3 T3-L1 adipocytes (Supplemental Fig. S2A). We observed that Gapex-5 knockdown only reduced insulin-stimulated glucose uptake at low doses of insulin (1 nM), whereas at high doses (100 nM), insulin-stimulated glucose uptake was not affected by Gapex-5 knockdown (Supplemental Fig. S2B), in contrast to previous reports [66]. In adipocytes, the effect of AMPK activation on glucose uptake remains unclear [68]. Since we also observed AMPK phosphorylation of Gapex-5 pSer902 in adipocytes (Supplemental Fig. S2C), it would be interesting to further investigate the effect of specific AMPK activation on glucose uptake in adipocytes and the potential involvement of Gapex-5 phosphorylation by AMPK.

Homozygous deletion of *gapvd1* in mouse is embryonically lethal (reported by the International Mouse Phenotyping Consortium for strain RRID:MMRRC_043884-UCD). Gapex-5 is highly conserved in zebrafish (78% protein identity, 86% similarity as assessed using NCBI blastp), with Ser896 corresponding to Ser902 in human Gapex-5 (Supplemental Fig. S3A). This has prompted us to generate Gapex-5 deficient zebrafish by introducing a frameshift mutation in the *gapvd1* gene using CRISPR/Cas9 (Supplemental Fig. S3B). Both heterozygous and homozygous carriers of the knockout allele were viable into adulthood (Supplemental Fig. S3C), however abnormal jaw and rough skin were observed with complete penetrance in adult knockout animals (Supplemental Fig. S3D). Using the tissue from Gapex-5 knockout zebrafish, we confirmed the identity of the immunoreactive band of 250 kDa as Gapex-5 (Supplemental Fig. S3E). Thus, having shown that Gapex-5 knockout zebrafish are viable opens the door for further studies of Gapex-5 in an animal model.

We also characterised a second protein identified in our screen, the glycogen-binding protein STBD1, showing AMPK-dependent phosphorylation on Ser175 (Figs. 3 and 4). AMPK binds glycogen through the carbohydrate binding module located in the regulatory β subunit [69–71], but the physiological role of AMPK binding to glycogen is not understood. A proposed role for AMPK in glycogen metabolism is inhibition of glycogen synthesis through direct phosphorylation of muscle and liver glycogen synthase [45,72,73], but it is unclear under which physiological conditions AMPK activation would lead to inhibition of glycogen synthesis [74]. STBD1 (also known as Genethonin 1 or GENX-3414) has been reported to bind glycogen [48,75,76], associate with the endoplasmic reticulum and mitochondria [77], and to interact with GABARAPL1, a member of the ATG8 family of proteins involved in autophagy [48,78]. Therefore, STBD1 has been proposed to play a role in glycophagy, a cellular process in which glycogen is transferred to the lysosome and degraded by lysosomal α-glucosidase (GAA). This pathway is defective in Pompe disease (glycogen storage disease type II; OMIM #232300), where GAA deficiency leads to severe accumulation of glycogen and damage to tissues [74]. Interestingly, GAA/STBD1 double knockout mice exhibited reduced accumulation of lysosomal glycogen in liver, but not in skeletal muscle [79]. To date, separate characterisation of the STBD1 knockout mouse has not been reported.

In the brain, glycogen is present at much lower amounts than in skeletal muscle and liver but has nonetheless been shown to have important functions [80]. Moreover, pathological accumulation of glycogen in neurons, such as in Lafora disease (OMIM #254780) results in neurodegeneration [81]. Although we didn't detect STBD1 in total brain lysates (Fig. 3A), STBD1 was detected in neuronal cell lines and AMPK activation increased phosphorylation of STBD1-Ser175 in these cells (Supplemental Fig. S4C). Whether AMPK phosphorylation of STBD1 represents an additional mechanism to regulate glycogen metabolism in different tissues such as liver, muscle or brain, remains to be determined.

There are several interesting hits identified in the current screen. For example, carnitine palmitoyltransferase 1 (CPT1) is an enzyme localised in the outer mitochondrial membrane that converts long-chain acyl-CoA species to their corresponding long-chain acyl-carnitines for

transport into the mitochondria for oxidation [2,82]. Given it is established that AMPK regulation of ACC controls the level of malonyl-CoA which in turn is a negative regulator of CPT1, it would be of interest to explore the role that AMPK has on CPT1 in terms of its functionality. In addition, AMP-deaminase (AMPD) is involved in regulation of energetic metabolism in mammalian cells and it catalyses conversion of AMP to IMP. AMPD inhibitors have been proposed as useful agents for boosting AMPK activation in cells and tissues during ATP-depletion [83]. In mouse liver, a loss of function study has demonstrated that AMPD2 plays an important role in maintaining metabolic/glucose homeostasis [84]. Whether AMPK has role in modulating AMPD2 activity is unknown, and this warrants future investigation.

Recent pre-clinical studies using novel small-molecule AMPK activators have shown that AMPK activators hold promise as glucose-lowering agents [18,19]. Exemplified by the cardiac hypertrophy encountered in one study [19], more work is nevertheless needed to understand the tissue-specific effects of chronic AMPK activation. To that end, our study describes a systematic approach for identification of direct AMPK targets and subsequent biochemical characterisation, which will advance our understanding of AMPK downstream action in a cell- or tissue-specific manner.

5. Conclusions

Here we report a chemical genetic screen for AMPK substrates in primary mouse hepatocytes and identify 65 proteins phosphorylated by ATP-analogue specific AMPK. We further established AMPK-dependent phosphorylation of endogenous Ser902-Gapex-5 in hepatocytes and Ser175-STBD1 in both hepatocytes and skeletal muscle. Further study of the functional importance of these phosphorylation events is however necessary. This study expands on our knowledge of AMPK downstream targets in hepatocytes.

Declaration of interest

S.D., M.D., C.C., P. G. and K.S. are employees of Nestlé Research (Switzerland).

Author contribution statement

S.D. and K.S. designed experiments, analysed the results and drafted the manuscript. S.D. performed most of the experiments and K.S supervised S.D. and overall study. M.D. performed molecular biology experiments (cloning, mutagenesis, DNA sequencing). D.S. performed mass spectrometry (MS) analysis and also provided interpretation of the MS-related results. M.F. and B.V. generated AMPK liver-specific double-knockout mouse model (AMPK DKO) and M.F. isolated and treated

AMPK DKO hepatocytes for biochemical analysis (performed by S.D.). A.B.M. and T.E.J. performed isolation and incubation of mouse skeletal muscle for biochemical analysis (performed by C.C.). O.G. performed silencing and glucose uptake experiments in 3 T3-L1 adipocytes. S.S. and A.Z. performed hepatocyte isolation and transfection for endocytosis assays and confocal microscopy analysis. S.D. and P.G. designed and generated the zebrafish model and performed experiments. All co-authors edited and approved the manuscript.

Appendix A. Supplementary data

Supplementary data to this article can be found online at https://doi.org/10.1016/j.cellsig.2019.02.001.

References

[1] G.R. Steinberg, B.E. Kemp, AMPK in Health and Disease, Physiol. Rev. 89 (3) (2009) 1025–1078.

[2] D.G. Hardie, K. Sakamoto, AMPK: a key sensor of fuel and energy status in skeletal muscle, Physiology 21 (2006) 48–60.

[3] D.G. Hardie, AMP-activated protein kinase: an energy sensor that regulates all aspects of cell function, Genes Dev. 25 (18) (2011) 1895–1908.

[4] D.G. Hardie, F.A. Ross, S.A. Hawley, AMPK: a nutrient and energy sensor that maintains energy homeostasis, Nat. Rev. Mol. Cell Biol. 13 (4) (2012) 251–262.

[5] D. Carling, C. Thornton, A. Woods, M.J. Sanders, AMP-activated protein kinase: new regulation, new roles? Biochem. J. 445 (1) (2012) 11–27.

[6] B.B. Kahn, T. Alquier, D. Carling, D.G. Hardie, AMP-activated protein kinase: ancient energy gauge provides clues to modern understanding of metabolism, Cell Metab. 1 (1) (2005) 15–25.

[7] D.G. Hardie, B.E. Schaffer, A. Brunet, AMPK: an energy-sensing pathway with multiple inputs and outputs, Trends Cell Biol. 26 (3) (2016) 190–201.

[8] G.F. Merrill, E.J. Kurth, D.G. Hardie, W.W. Winder, AICA riboside increases AMP-activated protein kinase, fatty acid oxidation, and glucose uptake in rat muscle, Am. J. Phys. 273 (6) (1997) E1107–E1112 Pt 1.

[9] D. Carling, V.A. Zammit, D.G. Hardie, A common bicyclic protein kinase cascade inactivates the regulatory enzymes of fatty acid and cholesterol biosynthesis, FEBS Lett. 223 (2) (1987) 217–222.

[10] Q. Chen, B. Xie, S. Zhu, P. Rong, Y. Sheng, S. Ducommun, L. Chen, C. Quan, M. Li, K. Sakamoto, C. MacKintosh, S. Chen, H.Y. Wang, A Tbc1d1 Ser231Ala-knockin mutation partially impairs AICAR- but not exercise-induced muscle glucose uptake in mice, Diabetologia 60 (2) (2017) 336–345.

[11] K. Sakamoto, G.D. Holman, Emerging role for AS160/TBC1D4 and TBC1D1 in the regulation of GLUT4 traffic, Am. J. Physiol. Endocrinol. Metab. 295 (1) (2008) E29–E37.

[12] D.M. Gwinn, D.B. Shackelford, D.F. Egan, M.M. Mihaylova, A. Mery, D.S. Vasquez, B.E. Turk, R.J. Shaw, AMPK phosphorylation of raptor mediates a metabolic checkpoint, Mol. Cell 30 (2) (2008) 214–226.

[13] E.Q. Toyama, S. Herzig, J. Courchet, T.L. Lewis Jr., O.C. Loson, K. Hellberg, N.P. Young, H. Chen, F. Polleux, D.C. Chan, R.J. Shaw, Metabolism. AMP-activated protein kinase mediates mitochondrial fission in response to energy stress, Science 351 (6270) (2016) 275–281.

[14] S. Ducommun, M. Deak, D. Sumpton, R.J. Ford, A. Nunez Galindo, M. Kussmann, B. Viollet, G.R. Steinberg, M. Foretz, L. Dayon, N.A. Morrice, K. Sakamoto, Motif affinity and mass spectrometry proteomic approach for the discovery of cellular AMPK targets: identification of mitochondrial fission factor as a new AMPK substrate, Cell. Signal. 27 (5) (2015) 978–988.

[15] E.P. Mottillo, E.M. Desjardins, J.D. Crane, B.K. Smith, A.E. Green, S. Ducommun, T.I. Henriksen, I.A. Rebalka, A. Razi, K. Sakamoto, C. Scheele, B.E. Kemp, T.J. Hawke, J. Ortega, J.G. Granneman, G.R. Steinberg, Lack of adipocyte AMPK exacerbates insulin resistance and hepatic Steatosis through Brown and Beige adipose tissue function, Cell Metab. 24 (1) (2016) 118–129.

[16] N.B. Ruderman, D. Carling, M. Prentki, J.M. Cacicedo, AMPK, insulin resistance, and the metabolic syndrome, J. Clin. Invest. 123 (7) (2013) 2764–2772.

[17] D.G. Hardie, F.A. Ross, S.A. Hawley, AMP-activated protein kinase: a target for drugs both ancient and modern, Chem. Biol. 19 (10) (2012) 1222–1236.

[18] E.C. Cokorinos, J. Delmore, A.R. Reyes, B. Albuquerque, R. Kjobsted, N.O. Jorgensen, J.L. Tran, A. Jatkar, K. Cialdea, R.M. Esquejo, J. Meissen, M.F. Calabrese, J. Cordes, R. Moccia, D. Tess, C.T. Salatto, T.M. Coskran, A.C. Opsahl, D. Flynn, M. Blatnik, W. Li, E. Kindt, M. Foretz, B. Viollet, J. Ward, R.G. Kurumbail, A.S. Kalgutkar, J.F.P. Wojtaszewski, K.O. Cameron, R.A. Miller, Activation of skeletal muscle AMPK promotes glucose disposal and glucose lowering in non-human Primates and mice, Cell Metab. 25 (5) (2017) 1147–1159 (e10).

[19] R.W. Myers, H.P. Guan, J. Ehrhart, A. Petrov, S. Prahalada, E. Tozzo, X. Yang, M.M. Kurtz, M. Trujillo, D. Gonzalez Trotter, D. Feng, S. Xu, G. Eiermann, M.A. Holahan, D. Rubins, S. Conarello, X. Niu, S.C. Souza, C. Miller, J. Liu, K. Lu, W. Feng, Y. Li, R.E. Painter, J.A. Milligan, H. He, F. Liu, A. Ogawa, D. Wisniewski, R.J. Rohm, L. Wang, M. Bunzel, Y. Qian, W. Zhu, H. Wang, B. Bennet, L. LaFranco Scheuch, G.E. Fernandez, C. Li, M. Klimas, G. Zhou, M. van Heek, T. Biftu, A. Weber, D.E. Kelley, N. Thornberry, M.D. Erion, D.M. Kemp, I.K. Sebhat, Systemic pan-AMPK activator MK-8722 improves glucose homeostasis but induces cardiac hypertrophy, Science 357 (6350) (2017) 507–511.

[20] M.R. Banko, J.J. Allen, B.E. Schaffer, E.W. Wilker, P. Tsou, J.L. White, J. Villen, B. Wang, S.R. Kim, K. Sakamoto, S.P. Gygi, L.C. Cantley, M.B. Yaffe, K.M. Shokat, A. Brunet, Chemical genetic screen for AMPKalpha2 substrates uncovers a network of proteins involved in mitosis, Mol. Cell 44 (6) (2011) 878–892.

[21] B.E. Schaffer, R.S. Levin, N.T. Hertz, T.J. Maures, M.L. Schoof, P.E. Hollstein, B.A. Benayoun, M.R. Banko, R.J. Shaw, K.M. Shokat, A. Brunet, Identification of AMPK phosphorylation sites reveals a network of proteins involved in cell invasion and facilitates large-scale substrate prediction, Cell Metab. 22 (5) (2015) 907–921.

[22] D.F. Egan, D.B. Shackelford, M.M. Mihaylova, S. Gelino, R.A. Kohnz, W. Mair, D.S. Vasquez, A. Joshi, D.M. Gwinn, R. Taylor, J.M. Asara, J. Fitzpatrick, A. Dillin, B. Viollet, M. Kundu, M. Hansen, R.J. Shaw, Phosphorylation of ULK1 (hATG1) by AMP-activated protein kinase connects energy sensing to mitophagy, Science 331 (6016) (2011) 456–461.

[23] K.O. Cameron, R.G. Kurumbail, Recent progress in the identification of adenosine monophosphate-activated protein kinase (AMPK) activators, Bioorg. Med. Chem. Lett. 26 (21) (2016) 5139–5148.

[24] D. Zibrova, F. Vandermoere, O. Goransson, M. Peggie, K.V. Marino, A. Knierim, K. Spengler, C. Weigert, B. Viollet, N.A. Morrice, K. Sakamoto, R. Heller, GFAT1 phosphorylation by AMPK promotes VEGF-induced angiogenesis, Biochem. J. 474 (6) (2017) 983–1001.

[25] B. Viollet, M. Foretz, B. Guigas, S. Horman, R. Dentin, L. Bertrand, L. Hue, F. Andreelli, Activation of AMP-activated protein kinase in the liver: a new strategy for the management of metabolic hepatic disorders, J. Physiol. 574 (Pt 1) (2006) 41–53.

[26] E.A. Richter, N.B. Ruderman, AMPK and the biochemistry of exercise: implications for human health and disease, Biochem. J. 418 (2) (2009) 261–275.

[27] C.S. Zhang, S.A. Hawley, Y. Zong, M. Li, Z. Wang, A. Gray, T. Ma, J. Cui, J.W. Feng, M. Zhu, Y.Q. Wu, T.Y. Li, Z. Ye, S.Y. Lin, H. Yin, H.L. Piao, D.G. Hardie, S.C. Lin, Fructose-1,6-bisphosphate and aldolase mediate glucose sensing by AMPK, Nature 548 (7665) (2017) 112–116.

[28] M. You, M. Matsumoto, C.M. Pacold, W.K. Cho, D.W. Crabb, The role of AMP-activated protein kinase in the action of ethanol in the liver, Gastroenterology 127 (6) (2004) 1798–1808.

[29] G. Zhou, R. Myers, Y. Li, Y. Chen, X. Shen, J. Fenyk-Melody, M. Wu, J. Ventre, T. Doebber, N. Fujii, N. Musi, M.F. Hirshman, L.J. Goodyear, D.E. Moller, Role of AMP-activated protein kinase in mechanism of metformin action, J. Clin. Invest. 108 (8) (2001) 1167–1174.

[30] R.W. Hunter, C.C. Hughey, L. Lantier, E.I. Sundelin, M. Peggie, E. Zeqiraj, F. Sicheri, N. Jessen, D.H. Wasserman, K. Sakamoto, Metformin reduces liver glucose production by inhibition of fructose-1-6-bisphosphatase, Nat. Med. 24 (9) (2018) 1395–1406.

[31] D. Grahame Hardie, Regulation of AMP-activated protein kinase by natural and synthetic activators, Acta Pharm. Sin. B 6 (1) (2016) 1–19.

[32] S.A. Hawley, M.D. Fullerton, F.A. Ross, J.D. Schertzer, C. Chevtzoff, K.J. Walker, M.W. Peggie, D. Zibrova, K.A. Green, K.J. Mustard, B.E. Kemp, K. Sakamoto, G.R. Steinberg, D.G. Hardie, The ancient drug salicylate directly activates AMP-activated protein kinase, Science 336 (6083) (2012) 918–922.

[33] X. Xia, J. Yan, Y. Shen, K. Tang, J. Yin, Y. Zhang, D. Yang, H. Liang, J. Ye, J. Weng, Berberine improves glucose metabolism in diabetic rats by inhibition of hepatic gluconeogenesis, PLoS ONE 6 (2) (2011) e16556.

[34] N. Boudaba, A. Marion, C. Huet, R. Pierre, B. Viollet, M. Foretz, AMPK re-activation suppresses hepatic Steatosis but its Downregulation does not promote fatty liver development, EBioMedicine 28 (2018) 194–209.

[35] J. Mu, J.T. Brozinick Jr., O. Valladares, M. Bucan, M.J. Birnbaum, A role for AMP-activated protein kinase in contraction- and hypoxia-regulated glucose transport in skeletal muscle, Mol. Cell 7 (5) (2001) 1085–1094.

[36] M. Foretz, S. Hebrard, J. Leclerc, E. Zarrinpashneh, M. Soty, G. Mithieux, K. Sakamoto, F. Andreelli, B. Viollet, Metformin inhibits hepatic gluconeogenesis in mice independently of the LKB1/AMPK pathway via a decrease in hepatic energy state, J. Clin. Invest. 120 (7) (2010) 2355–2369.

[37] R.W. Hunter, M. Foretz, L. Bultot, M.D. Fullerton, M. Deak, F.A. Ross, S.A. Hawley, N. Shpiro, B. Viollet, D. Barron, B.E. Kemp, G.R. Steinberg, D.G. Hardie, K. Sakamoto, Mechanism of action of compound-13: an alpha1-selective small molecule activator of AMPK, Chem. Biol. 21 (7) (2014) 866–879.

[38] T.E. Jensen, L. Sylow, A.J. Rose, A.B. Madsen, Y. Angin, S.J. Maarbjerg, E.A. Richter, Contraction-stimulated glucose transport in muscle is controlled by AMPK and mechanical stress but not sarcoplasmatic reticulum Ca(2+) release, Mol. Metab. 3 (7) (2014) 742–753.

[39] A. Keller, A.I. Nesvizhskii, E. Kolker, R. Aebersold, Empirical statistical model to estimate the accuracy of peptide identifications made by MS/MS and database search, Anal. Chem. 74 (20) (2002) 5383–5392.

[40] J.J. Allen, M. Li, C.S. Brinkworth, J.L. Paulson, D. Wang, A. Hubner, W.H. Chou, R.J. Davis, A.L. Burlingame, R.O. Messing, C.D. Katayama, S.M. Hedrick, K.M. Shokat, A semisynthetic epitope for kinase substrates, Nat. Methods 4 (6) (2007) 511–6.

[41] L. Bultot, T.E. Jensen, Y.C. Lai, A.L. Madsen, C. Collodet, S. Kviklyte, M. Deak, A. Yavari, M. Foretz, S. Ghaffari, M. Bellahcene, H. Ashrafian, M.H. Rider, E.A. Richter, K. Sakamoto, Benzimidazole derivative small-molecule 991 enhances AMPK activity and glucose uptake induced by AICAR or contraction in skeletal muscle, Am. J. Physiol. Endocrinol. Metab. 311 (4) (2016) E706–E719.

[42] B. Xiao, M.J. Sanders, D. Carmena, N.J. Bright, L.F. Haire, E. Underwood, B.R. Patel, R.B. Heath, P.A. Walker, S. Hallen, F. Giordanetto, S.R. Martin, D. Carling, S.J. Gamblin, Structural basis of AMPK regulation by small molecule activators, Nat. Commun. 4 (2013) 3017.

[43] K. Sakamoto, A. McCarthy, D. Smith, K.A. Green, D. Grahame Hardie, A. Ashworth, D.R. Alessi, Deficiency of LKB1 in skeletal muscle prevents AMPK activation and

glucose uptake during contraction, EMBO J. 24 (10) (2005) 1810–1820.

[44] R.W. Hunter, J.T. Treebak, J.F. Wojtaszewski, K. Sakamoto, Molecular mechanism by which AMP-activated protein kinase activation promotes glycogen accumulation in muscle, Diabetes 60 (3) (2011) 766–774.

[45] L. Bultot, B. Guigas, A. Von Wilamowitz-Moellendorff, L. Maisin, D. Vertommen, N. Hussain, M. Beullens, J.J. Guinovart, M. Foretz, B. Viollet, K. Sakamoto, L. Hue, M.H. Rider, AMP-activated protein kinase phosphorylates and inactivates liver glycogen synthase, Biochem. J. 443 (1) (2012) 193–203.

[46] M. Kim, R.W. Hunter, L. Garcia-Menendez, G. Gong, Y.Y. Yang, S.C. Kolwicz Jr., J. Xu, K. Sakamoto, W. Wang, R. Tian, Mutation in the gamma2-subunit of AMP-activated protein kinase stimulates cardiomyocyte proliferation and hypertrophy independent of glycogen storage, Circ. Res. 114 (6) (2014) 966–975.

[47] S. Ducommun, R.J. Ford, L. Bultot, M. Deak, L. Bertrand, B.E. Kemp, G.R. Steinberg, K. Sakamoto, Enhanced activation of cellular AMPK by dual-small molecule treat- ment: AICAR and A769662, Am. J. Physiol. Endocrinol. Metab. 306 (6) (2014) E688–E696.

[48] S. Jiang, B. Heller, V.S. Tagliabracci, L. Zhai, J.M. Irimia, A.A. DePaoli-Roach, C.D. Wells, A.V. Skurat, P.J. Roach, Starch binding domain-containing protein 1/ genethonin 1 is a novel participant in glycogen metabolism, J. Biol. Chem. 285 (45) (2010) (34960–71).

[49] N.J. Hoffman, B.L. Parker, R. Chaudhuri, K.H. Fisher-Wellman, M. Kleinert, S.J. Humphrey, P. Yang, M. Holliday, S. Trefely, D.J. Fazakerley, J. Stockli, J.G. Burchfield, T.E. Jensen, R. Jothi, B. Kiens, J.F. Wojtaszewski, E.A. Richter, D.E. James, Global Phosphoproteomic analysis of human skeletal muscle reveals a network of exercise-regulated kinases and AMPK substrates, Cell Metab. 22 (5) (2015) 922–935.

[50] J. Fentz, R. Kjobsted, J.B. Birk, A.B. Jordy, J. Jeppesen, K. Thorsen, P. Schjerling, B. Kiens, N. Jessen, B. Viollet, J.F. Wojtaszewski, AMPKalpha is critical for en- hancing skeletal muscle fatty acid utilization during in vivo exercise in mice, FASEB J. 29 (5) (2015) 1725–1738.

[51] D.D. Habets, W.A. Coumans, M. El Hasnaoui, E. Zarrinpashneh, L. Bertrand, B. Viollet, B. Kiens, T.E. Jensen, E.A. Richter, A. Bonen, J.F. Glatz, J.J. Luiken, Crucial role for LKB1 to AMPKalpha2 axis in the regulation of CD36-mediated long- chain fatty acid uptake into cardiomyocytes, Biochim. Biophys. Acta 1791 (3) (2009) (212–9).

[52] J.J. Luiken, S.L. Coort, J. Willems, W.A. Coumans, A. Bonen, G.J. van der Vusse, J.F. Glatz, Contraction-induced fatty acid translocase/CD36 translocation in rat cardiac myocytes is mediated through AMP-activated protein kinase signaling, Diabetes 52 (7) (2003) 1627–1634.

[53] J. Shearer, P.T. Fueger, B. Vorndick, D.P. Bracy, J.N. Rottman, J.A. Clanton, D.H. Wasserman, AMP kinase-induced skeletal muscle glucose but not long-chain fatty acid uptake is dependent on nitric oxide, Diabetes 53 (6) (2004) 1429–1435.

[54] T. Hayashi, M.F. Hirshman, E.J. Kurth, W.W. Winder, L.J. Goodyear, Evidence for 5' AMP-activated protein kinase mediation of the effect of muscle contraction on glucose transport, Diabetes 47 (8) (1998) 1369–1373.

[55] R. Bergeron, R.R. Russell 3rd, L.H. Young, J.M. Ren, M. Marcucci, A. Lee, G.I. Shulman, Effect of AMPK activation on muscle glucose metabolism in conscious rats, Am. J. Phys. 276 (5) (1999) E938–E944 Pt 1.

[56] S. Chen, J. Murphy, R. Toth, D.G. Campbell, N.A. Morrice, C. Mackintosh, Complementary regulation of TBC1D1 and AS160 by growth factors, insulin and AMPK activators, Biochem. J. 409 (2) (2008) 449–459.

[57] C. Pehmoller, J.T. Treebak, J.B. Birk, S. Chen, C. Mackintosh, D.G. Hardie, E.A. Richter, J.F. Wojtaszewski, Genetic disruption of AMPK signaling abolishes both contraction- and insulin-stimulated TBC1D1 phosphorylation and 14-3-3 binding in mouse skeletal muscle, Am. J. Physiol. Endocrinol. Metab. 297 (3) (2009) E665–E675.

[58] D. An, T. Toyoda, E.B. Taylor, H. Yu, N. Fujii, M.F. Hirshman, L.J. Goodyear, TBC1D1 regulates insulin- and contraction-induced glucose transport in mouse skeletal muscle, Diabetes 59 (6) (2010) 1358–1365.

[59] N. Wu, B. Zheng, A. Shaywitz, Y. Dagon, C. Tower, G. Bellinger, C.H. Shen, J. Wen, J. Asara, T.E. McGraw, B.B. Kahn, L.C. Cantley, AMPK-dependent degradation of TXNIP upon energy stress leads to enhanced glucose uptake via GLUT1, Mol. Cell 49 (6) (2013) 1167–1175.

[60] C.M. Hunker, A. Galvis, I. Kruk, H. Giambini, M.L. Veisaga, M.A. Barbieri, Rab5- activating protein 6, a novel endosomal protein with a role in endocytosis, Biochem. Biophys. Res. Commun. 340 (3) (2006) 967–975.

[61] X. Su, C. Kong, P.D. Stahl, GAPex-5 mediates ubiquitination, trafficking, and de- gradation of epidermal growth factor receptor, J. Biol. Chem. 282 (29) (2007) 21278–21284.

[62] X. Su, I.J. Lodhi, A.R. Saltiel, P.D. Stahl, Insulin-stimulated interaction between insulin receptor substrate 1 and p85alpha and activation of protein kinase B/Akt require Rab5, J. Biol. Chem. 281 (38) (2006) 27982–27990.

[63] A. Zeigerer, J. Gilleron, R.L. Bogorad, G. Marsico, H. Nonaka, S. Seifert, H. Epstein- Barash, S. Kuchimanchi, C.G. Peng, V.M. Ruda, P. Del Conte-Zerial, J.G. Hengstler, Y. Kalaidzidis, V. Koteliansky, M. Zerial, Rab5 is necessary for the biogenesis of the endolysosomal system in vivo, Nature 485 (7399) (2012) 465–470.

[64] J.D. Orth, E.W. Krueger, S.G. Weller, M.A. McNiven, A novel endocytic mechanism of epidermal growth factor receptor sequestration and internalization, Cancer Res. 66 (7) (2006) (3603–10).

[65] S. Sigismund, T. Woelk, C. Puri, E. Maspero, C. Tacchetti, P. Transidico, P.P. Di Fiore, S. Polo, Clathrin-independent endocytosis of ubiquitinated cargos, Proc. Natl. Acad. Sci. U. S. A. 102 (8) (2005) (2760–5).

[66] I.J. Lodhi, D. Bridges, S.H. Chiang, Y. Zhang, A. Cheng, L.M. Geletka, L.S. Weisman, A.R. Saltiel, Insulin stimulates phosphatidylinositol 3-phosphate production via the activation of Rab5, Mol. Biol. Cell 19 (7) (2008) 2718–2728.

[67] I.J. Lodhi, S.H. Chiang, L. Chang, D. Vollenweider, R.T. Watson, M. Inoue, J.E. Pessin, A.R. Saltiel, Gapex-5, a Rab31 guanine nucleotide exchange factor that regulates Glut4 trafficking in adipocytes, Cell Metab. 5 (1) (2007) 59–72.

[68] S. Bijland, S.J. Mancini, I.P. Salt, Role of AMP-activated protein kinase in adipose tissue metabolism and inflammation, Clin. Sci. (Lond.) 124 (8) (2013) 491–507.

[69] E.R. Hudson, D.A. Pan, J. James, J.M. Lucocq, S.A. Hawley, K.A. Green, O. Baba, T. Terashima, D.G. Hardie, A novel domain in AMP-activated protein kinase causes glycogen storage bodies similar to those seen in hereditary cardiac arrhythmias, Curr. Biol. 13 (10) (2003) (861–6).

[70] G. Polekhina, A. Gupta, B.J. Michell, B. van Denderen, S. Murthy, S.C. Feil, I.G. Jennings, D.J. Campbell, L.A. Witters, M.W. Parker, B.E. Kemp, D. Stapleton, AMPK beta subunit targets metabolic stress sensing to glycogen, Curr. Biol. 13 (10) (2003) 867–871.

[71] Y. Oligschlaeger, M. Miglianico, D. Chanda, R. Scholz, R.F. Thali, R. Tuerk, D.I. Stapleton, P.R. Gooley, D. Neumann, The recruitment of AMP-activated protein kinase to glycogen is regulated by autophosphorylation, J. Biol. Chem. 290 (18) (2015) 11715–11728.

[72] D. Carling, D.G. Hardie, The substrate and sequence specificity of the AMP-acti- vated protein kinase. Phosphorylation of glycogen synthase and phosphorylase ki- nase, Biochim. Biophys. Acta 1012 (1) (1989) (81–6).

[73] S.B. Jorgensen, J.N. Nielsen, J.B. Birk, G.S. Olsen, B. Viollet, F. Andreelli, P. Schjerling, S. Vaulont, D.G. Hardie, B.F. Hansen, E.A. Richter, J.F. Wojtaszewski, The alpha2-5'AMP-activated protein kinase is a site 2 glycogen synthase kinase in skeletal muscle and is responsive to glucose loading, Diabetes 53 (12) (2004) 3074–3081.

[74] P.J. Roach, A.A. Depaoli-Roach, T.D. Hurley, V.S. Tagliabracci, Glycogen and its metabolism: some new developments and old themes, Biochem. J. 441 (3) (2012) 763–787.

[75] D. Stapleton, C. Nelson, K. Parsawar, D. McClain, R. Gilbert-Wilson, E. Barker, B. Rudd, K. Brown, W. Hendrix, P. O'Donnell, G. Parker, Analysis of hepatic gly- cogen-associated proteins, Proteomics 10 (12) (2010) (2320–9).

[76] S. Bouju, M.F. Lignon, G. Pietu, M. Le Cunff, J.J. Leger, C. Auffray, C.A. Dechesne, Molecular cloning and functional expression of a novel human gene encoding two 41-43 kDa skeletal muscle internal membrane proteins, Biochem. J. 335 (1998) 549–556 Pt 3.

[77] A. Demetriadou, J. Morales-Sanfrutos, M. Nearchou, O. Baba, K. Kyriacou, E.W. Tate, A. Drousiotou, P.P. Petrou, Mouse Stbd1 is N-myristoylated and affects ER-mitochondria association and mitochondrial morphology, J. Cell Sci. 130 (5) (2017) 903–915.

[78] S. Jiang, C.D. Wells, P.J. Roach, Starch-binding domain-containing protein 1 (Stbd1) and glycogen metabolism: identification of the Atg8 family interacting motif (AIM) in Stbd1 required for interaction with GABARAPL1, Biochem. Biophys. Res. Commun. 413 (3) (2011) (420–5).

[79] T. Sun, H. Yi, C. Yang, P.S. Kishnani, B. Sun, Starch binding domain-containing protein 1 plays a dominant role in glycogen transport to lysosomes in liver, J. Biol. Chem. 291 (32) (2016) 16479–16484.

[80] J. Duran, J.J. Guinovart, Brain glycogen in health and disease, Mol. Asp. Med. 46 (2015) 7–70.

[81] P.J. Roach, Glycogen phosphorylation and Lafora disease, Mol. Asp. Med. 46 (2015) 78–84.

[82] B.K. Smith, G.R. Steinberg, AMP-activated protein kinase, fatty acid metabolism, and insulin sensitivity, Curr. Opin. Clin. Nutr. Metab. Care 20 (4) (2017) 248–253.

[83] C. Plaideau, Y.C. Lai, S. Kviklyte, N. Zanou, L. Lofgren, H. Andersen, D. Vertommen, P. Gailly, L. Hue, Y.M. Bohlooly, S. Hallen, M.H. Rider, Effects of pharmacological AMP deaminase inhibition and Ampd1 deletion on nucleotide levels and AMPK activation in contracting skeletal muscle, Chem. Biol. 21 (11) (2014) 1497–1510.

[84] A.W. Hudoyo, T. Hirase, A. Tandelillin, M. Honda, M. Shirai, J. Cheng, H. Morisaki, T. Morisaki, Role of AMPD2 in impaired glucose tolerance induced by high fructose diet, Mol. Genet. Metab. Rep. 13 (2017) 23–29.

[85] S.P. Davies, D. Carling, M.R. Munday, D.G. Hardie, Diurnal rhythm of phosphor- ylation of rat liver acetyl-CoA carboxylase by the AMP-activated protein kinase, demonstrated using freeze-clamping. Effects of high fat diets, Eur. J. Biochem. 203 (3) (1992) 615–623.

[86] L. Abu-Elheiga, D.B. Almarza-Ortega, A. Baldini, S.J. Wakil, Human acetyl-CoA carboxylase 2. Molecular cloning, characterization, chromosomal mapping, and evidence for two isoforms, J. Biol. Chem. 272 (16) (1997) 10669–10677.